interactions are epistatic (Ueta et al., 2012b). Based on the findings discussed here we strongly suspect that the lack of balance between TLR3 and EP3 can trigger ocular surface inflammation (Fig. 22).

7. Conclusions and future directions

In this review we raise the possibility that some ocular surface inflammatory diseases are pathogenetically related with a disordered innate immune response.

Although the ocular surface epithelium is in constant contact with bacteria and bacterial products, the healthy ocular surface is not in an inflammatory state. The balance between the mucosal immunity of the ocular surface and the pathogenicity of bacteria is very important. We suspect that when the host mucosal immunity is normal, commensal bacteria are in a symbiotic relationship with their host, however, if the host mucosal immunity is abnormal, commensal bacteria may become pathogenic. Some ocular surface inflammatory diseases such as catarrhal ulcers and phlyctenular keratitis are considered to be hypersensitivity to bacteria.

We also showed that although immune-competent cells such as macrophages could recognize various microbial components through various TLRs, induce inflammation and then exclude the microbes, ocular surface epithelial cells can selectively respond to microbial components and induce limited inflammation. We suspect that the difference between ocular surface epithelial cells and macrophages lies in their dissimilarity with respect to their coexistence with commensal bacteria. The unique innate immune response machinery of the ocular surface epithelium may explain the permissive coexistence with commensal bacteria. We also document that human ocular surface epithelial cells can be induced upon stimulation with polyI:C, a ligand of TLR3, RIG-I and MDA-5, to express many transcripts including not only anti-viral innate immune response-related- but also allergy-related-genes.

We provided evidence that allergic eosinophilic infiltration of the conjunctiva can be regulated by conjunctival epithelial cells through EP3 and TLR3.

Our findings indicate that disordered innate immunity can induce ocular surface inflammation because mice in which IκBζ was knocked out, expressly exhibited severe, spontaneous ocular surface inflammation with the eventual loss of almost all goblet cells.

Lastly we suggest that the pathogenesis of SJS with severe ocular surface complications, a devastating severe ocular surface inflammatory disease, is associated with innate immune reaction abnomalies, especially those related with the epistatic interactions between TLR3 and EP3. Thus, the lack of balance between TLR3 and EP3 might trigger ocular surface inflammation.

Focusing on the innate immunity of the ocular surface might help to elucidate the pathogenesis of various ocular surface diseases (Fig. 23).

References

Abe, R., Shimizu, T., Shibaki, A., Nakamura, H., Watanabe, H., Shimizu, H., 2003. Toxic epidermal necrolysis and Stevens-Johnson syndrome are induced by soluble Fas ligand. American Journal of Pathology 162, 1515–1520.

Alexopoulou, L., Holt, A.C., Medzhitov, R., Flavell, R.A., 2001. Recognition of double-stranded RNA and activation of NF-kappaB by Toll-like receptor 3. Nature 413, 732–738.

Auquier-Dunant, A., Mockenhaupt, M., Naldi, L., Correia, O., Schroder, W., Roujeau, J.C., 2002. Correlations between clinical patterns and causes of erythema multiforme majus, Stevens-Johnson syndrome, and toxic epidermal necrolysis: results of an international prospective study. Archives of Dermatology 138, 1019–1024.

Baum, J.L., 1978. Current concepts in ophthalmology. Ocular infections. The New England Journal of Medicine 299, 28–31.

Beauchamp, G.R., Gillette, T.E., Friendly, D.S., 1981. Phlyctenular keratoconjunctivitis. Journal of Pediatric Ophthalmology and Strabismus 18, 22–28.

Bouma, G., Strober, W., 2003. The immunological and genetic basis of inflammatory bowel disease. Nature Reviews Immunology 3, 521–533.

Broide, D.H., 2007. The pathophysiology of allergic rhinoconjunctivitis. Allergy and Asthma Proceedings: the Official Journal of Regional and State Allergy Societies 28, 398–403.

Bullens, D.M., Decraene, A., Dilissen, E., Meyts, I., De Boeck, K., Dupont, L.J., Ceuppens, J.L., 2008. Type III IFN-lambda mRNA expression in sputum of adult and school-aged asthmatics. Clinical and Experimental Allergy 38, 1459–1467.

Cavassani, K.A., Ishii, M., Wen, H., Schaller, M.A., Lincoln, P.M., Lukacs, N.W., Hogaboam, C.M., Kunkel, S.L., 2008. TLR3 is an endogenous sensor of tissue necrosis during acute inflammatory events. The Journal of Experimental Medicine 205, 2609–2621.

Cho, J.H., 2008. The genetics and immunopathogenesis of inflammatory bowel disease. Nature Reviews Immunology 8, 458–466.

Chung, W.H., Hung, S.I., Hong, H.S., Hsih, M.S., Yang, L.C., Ho, H.C., Wu, J.Y., Chen, Y.T., 2004. Medical genetics: a marker for Stevens-Johnson syndrome. Nature 428, 486.

Cordell, H.J., 2009. Detecting gene-gene interactions that underlie human diseases. Nature Reviews Genetics 10, 392–404.

Correia, O., Delgado, L., Roujeau, J.C., Le Cleach, L., Fleming-Torrinha, J.A., 2002. Soluble interleukin 2 receptor and interleukin 1alpha in toxic epidermal necrolysis: a comparative analysis of serum and blister fluid samples. Archives of Dermatology 138, 29–32.

Doyle, A., Beigi, B., Early, A., Blake, A., Eustace, P., Hone, R., 1995. Adherence of bacteria to intraocular lenses: a prospective study. The British Journal of Ophthalmology 79, 347–349.

Farber, J.M., 1997. Mig and IP-10: CXC chemokines that target lymphocytes. Journal of Leukocyte Biology 61, 246–257.

Ficker, L., Seal, D., Wright, P., 1989. Staphylococcal infection and the limbus: study of the cell-mediated immune response. Eye (Lond) 3, 190–193.

Forman, R., Koren, G., Shear, N.H., 2002. Erythema multiforme, Stevens-Johnson syndrome and toxic epidermal necrolysis in children: a review of 10 years' experience. Drug Safety 25, 965–972.

Fukuda, K., Kumagai, N., Fujitsu, Y., Nishida, T., 2006. Fibroblasts as local immune modulators in ocular allergic disease. Allergology International 55, 121–129.

Fukushima, A., 2007. Roles of T-cells in the development of allergic conjunctival diseases. Cornea 26, S36–S40.

Graziano, F.M., Stahl, J.L., Cook, E.B., Barney, N.P., 2001. Conjunctival mast cells in ocular allergic disease. Allergy Asthma Proc 22, 121–126.

Gros, E., Bussmann, C., Bieber, T., Forster, I., Novak, N., 2009. Expression of chemokines and chemokine receptors in lesional and nonlesional upper skin of patients with atopic dermatitis. The Journal of Allergy and Clinical Immunology.

Hallen, L.C., Burki, Y., Ebeling, M., Broger, C., Siegrist, F., Oroszlan-Szovik, K., Bohrmann, B., Certa, U., Foser, S., 2007. Antiproliferative activity of the human IFN-alpha-inducible protein IFI44. J Interferon Cytokine Res 27, 675–680.

Hara, J., Yasuda, F., Higashitsutsumi, M., 1997. Preoperative disinfection of the conjunctival sac in cataract surgery. Ophthalmologica. Journal International D'ophtalmologie. International Journal of Ophthalmology. Zeitschrift fur Augenheilkunde 211 (Suppl. 1), 62–67.

Haynes, R.J., Tighe, P.J., Dua, H.S., 1999. Antimicrobial defensin peptides of the human ocular surface. The British Journal of Ophthalmology 83, 737–741.

Heinzmann, A., Mao, X.Q., Akaiwa, M., Kreomer, R.T., Gao, P.S., Ohshima, K., Umeshita, R., Abe, Y., Braun, S., Yamashita, T., Roberts, M.H., Sugimoto, R., Arima, K., Arinobu, Y., Yu, B., Kruse, S., Enomoto, T., Dake, Y., Kawai, M., Shimazu, S., Sasaki, S., Adra, C.N., Kitaichi, M., Inoue, H., Yamauchi, K., Tomichi, N., Kurimoto, F., Hamasaki, N., Hopkin, J.M., Izuhara, K., Shirakawa, T., Deichmann, K.A., 2000. Genetic variants of IL-13 signalling and human asthma and atopy. Human Molecular Genetics 9, 549–559.

Hingorani, M., Calder, V.L., Buckley, R.J., Lightman, S.L., 1998. The role of conjunctival epithelial cells in chronic ocular allergic disease. Experimental Eye Research 67, 491–500.

Honda, T., Matsuoka, T., Ueta, M., Kabashima, K., Miyachi, Y., Narumiya, S., 2009. Prostaglandin E(2)-EP(3) signaling suppresses skin inflammation in murine contact hypersensitivity. The Journal of Allergy and Clinical Immunology 124, 809–818. e802.

Horisberger, M.A., 1995. Interferons, Mx genes, and resistance to influenza virus. American Journal of Respiratory and Critical Care Medicine 152, S67–S71.

Hornung, V., Rothenfusser, S., Britsch, S., Krug, A., Jahrsdorfer, B., Giese, T., Endres, S., Hartmann, G., 2002. Quantitative expression of toll-like receptor 1-10 mRNA in cellular subsets of human peripheral blood mononuclear cells and sensitivity to CpG oligodeoxynucleotides. The Journal of Immunology 168, 4531–4537.

Hozono, Y., Ueta, M., Hamuro, J., Kojima, K., Kawasaki, S., Yamazaki, K., Kinoshita, S., 2006. Human corneal epithelial cells respond to ocular-pathogenic, but not to nonpathogenic-flagellin. Biochemical and Biophysical Research Communications 347, 238–247.

Hung, S.I., Chung, W.H., Liou, L.B., Chu, C.C., Lin, M., Huang, H.P., Lin, Y.L., Lan, J.L., Yang, L.C., Hong, H.S., Chen, M.J., Lai, P.C., Wu, M.S., Chu, C.Y., Wang, K.H., Chen, C.H., Fann, C.S., Wu, J.Y., Chen, Y.T., 2005. HLA-B*5801 allele as a genetic marker for severe cutaneous adverse reactions caused by allopurinol. Proceedings of the National Academy of Sciences of the United States of America 102, 4134–4139.

Jin, H.K., Yoshimatsu, K., Takada, A., Ogino, M., Asano, A., Arikawa, J., Watanabe, T., 2001. Mouse Mx2 protein inhibits hantavirus but not influenza virus replication. Archives of Virology 146, 41–49.

Please cite this article in press as: Ueta, M., Kinoshita, S., Ocular surface inflammation is regulated by innate immunity, Progress in Retinal and Eye Research (2012), http://dx.doi.org/10.1016/j.preteyeres.2012.05.003

Johnson, A.C., Heinzel, F.P., Diaconu, E., Sun, Y., Hise, A.G., Golenbock, D., Lass, J.H., Pearlman, E., 2005. Activation of toll-like receptor (TLR)2, TLR4, and TLR9 in the mammalian cornea induces MyD88-dependent corneal inflammation. Investigative Ophthalmology & Visual Science 46, 589–595.

Kaniwa, N., Saito, Y., Aihara, M., Matsunaga, K., Tohkin, M., Kurose, K., Sawada, J., Furuya, H., Takahashi, Y., Muramatsu, M., Kinoshita, S., Abe, M., Ikeda, H., Kashiwagi, M., Song, Y., Ueta, M., Sotozono, C., Ikezawa, Z., Hasegawa, R., 2008. HLA-B locus in Japanese patients with anti-epileptics and allopurinol-related Stevens-Johnson syndrome and toxic epidermal necrolysis. Pharmacogenomics 9, 1617–1622.

Kato, A., Favoreto Jr., S., Avila, P.C., Schleimer, R.P., 2007. TLR3- and Th2 cytokine-dependent production of thymic stromal lymphopoietin in human airway epithelial cells. The Journal of Immunology 179, 1080–1087.

Kawai, T., Akira, S., 2007. TLR signaling. Seminars in Immunology 19, 24–32.

Kawai, T., Akira, S., 2009. The roles of TLRs, RLRs and NLRs in pathogen recognition. International Immunology 21, 317–337.

Kawai, T., Takahashi, K., Sato, S., Coban, C., Kumar, H., Kato, H., Ishii, K.J., Takeuchi, O., Akira, S., 2005. IPS-1, an adaptor triggering RIG-I- and Mda5-mediated type I interferon induction. Nature Immunology 6, 981–988.

Kinoshita, H., Takai, T., Le, T.A., Kamijo, S., Wang, X.L., Ushio, H., Hara, M., Kawasaki, J., Vu, A.T., Ogawa, T., Gunawan, H., Ikeda, S., Okumura, K., Ogawa, H., 2008. Cytokine milieu modulates release of thymic stromal lymphopoietin from human keratinocytes stimulated with double-stranded RNA. The Journal of Allergy and Clinical Immunology.

Kloos, W.E., Musselwhite, M.S., 1975. Distribution and persistence of *Staphylococcus* and *Micrococcus* species and other aerobic bacteria on human skin. Applied Microbiology 30, 381–385.

Klunker, S., Trautmann, A., Akdis, M., Verhagen, J., Schmid-Grendelmeier, P., Blaser, K., Akdis, C.A., 2003. A second step of chemotaxis after transendothelial migration: keratinocytes undergoing apoptosis release IFN-gamma-inducible protein 10, monokine induced by IFN-gamma, and IFN-gamma-inducible alpha-chemoattractant for T cell chemotaxis toward epidermis in atopic dermatitis. The Journal of Immunology 171, 1078–1084.

Kojima, K., Ueta, M., Hamuro, J., Hozono, Y., Kawasaki, S., Yokoi, N., Kinoshita, S., 2008. Human conjunctival epithelial cells express functional Toll-like receptor 5. The British Journal of Ophthalmology 92, 411–416.

Kumar, A., Zhang, J., Yu, F.S., 2006. Toll-like receptor 3 agonist poly(I: C)-induced antiviral response in human corneal epithelial cells. Immunology 117, 11–21.

Kumar, A., Yin, J., Zhang, J., Yu, F.S., 2007. Modulation of corneal epithelial innate immune response to pseudomonas infection by flagellin pretreatment. Investigative Ophthalmology & Visual Science 48, 4664–4670.

Kunikata, T., Yamane, H., Segi, E., Matsuoka, T., Sugimoto, Y., Tanaka, S., Tanaka, H., Nagai, H., Ichikawa, A., Narumiya, S., 2005. Suppression of allergic inflammation by the prostaglandin E receptor subtype EP3. Nature Immunology 6, 524–531.

Leaute-Labreze, C., Lamireau, T., Chawki, D., Maleville, J., Taieb, A., 2000. Diagnosis, classification, and management of erythema multiforme and Stevens-Johnson syndrome. Archives of Disease in Childhood 83, 347–352.

Levi, N., Bastuji-Garin, S., Mockenhaupt, M., Roujeau, J.C., Flahault, A., Kelly, J.P., Martin, E., Kaufman, D.W., Maison, P., 2009. Medications as risk factors of Stevens-Johnson syndrome and toxic epidermal necrolysis in children: a pooled analysis. Pediatrics 123, e297–304.

Lonjou, C., Thomas, L., Borot, N., Ledger, N., de Toma, C., LeLouet, H., Graf, E., Schumacher, M., Hovnanian, A., Mockenhaupt, M., Roujeau, J.C., 2006. A marker for Stevens-Johnson syndrome: ethnicity matters. The Pharmacogenomics Journal 6, 265–268.

Lonjou, C., Borot, N., Sekula, P., Ledger, N., Thomas, L., Halevy, S., Naldi, L., Bouwes-Bavinck, J.N., Sidoroff, A., de Toma, C., Schumacher, M., Roujeau, J.C., Hovnanian, A., Mockenhaupt, M., 2008. A European study of HLA-B in Stevens-Johnson syndrome and toxic epidermal necrolysis related to five high-risk drugs. Pharmacogenet Genomics 18, 99–107.

Medzhitov, R., Preston-Hurlburt, P., Janeway Jr., C.A., 1997. A human homologue of the Drosophila Toll protein signals activation of adaptive immunity. Nature 388, 394–397.

Miyairi, I., Tatireddigari, V.R., Mahdi, O.S., Rose, L.A., Belland, R.J., Lu, L., Williams, R.W., Byrne, G.I., 2007. The p47 GTPases Iigp2 and Irgb10 regulate innate immunity and inflammation to murine Chlamydia psittaci infection. The Journal of Immunology 179, 1814–1824.

Mockenhaupt, M., Viboud, C., Dunant, A., Naldi, L., Halevy, S., Bouwes Bavinck, J.N., Sidoroff, A., Schneck, J., Roujeau, J.C., Flahault, A., 2008. Stevens-Johnson syndrome and toxic epidermal necrolysis: assessment of medication risks with emphasis on recently marketed drugs. The EuroSCAR-study. The Journal of Investigative Dermatology 128, 35–44.

Mondini, M., Costa, S., Sponza, S., Gugliesi, F., Gariglio, M., Landolfo, S., 2010. The interferon-inducible HIN-200 gene family in apoptosis and inflammation: implication for autoimmunity. Autoimmunity 43, 226–231.

Mondino, B.J., Kowalski, R., 1982. Phlyctenulae and catarrhal infiltrates-occurrence in rabbits immunised with staphylococcal cell walls. Archives of Ophthalmology 100, 1968–1971.

Mondino, B.J., Brown, S.I., Rabin, B.S., 1978. Role of complement in corneal inflammation. Transactions of the Ophthalmological Societies of the United Kingdom 98, 363–366.

Mondino, B.J., Kowalski, R., Ratajczak, H.V., Petes, J., Cutler, S.B., Bronw, S.I., 1981. Rabbit model of phlyctenulosis and catarrhal infiltrates. Archives of Ophthalmology 99, 891–895.

Mondino, B.J., Brown, S.I., Biglan, A.W., 1982. HLA antigens in Stevens-Johnson syndrome with ocular involvement. Archives of Ophthalmology 100, 1453–1454.

Narumiya, S., Sugimoto, Y., Ushikubi, F., 1999. Prostanoid receptors: structures, properties, and functions. Physiol Rev 79, 1193–1226.

Neiberg, M.N., Sowka, J., 2008. Phlyctenular keratoconjunctivitis in a patient with Staphylococcal blepharitis and ocular rosacea. Optometry 79, 133–137.

Ohji, M., Ohmi, G., Kiritoshi, A., Kinoshita, S., 1987. Goblet cell density in thermal and chemical injuries. Archives of Ophthalmology 105, 1686–1688.

Ono, S.J., Abelson, M.B., 2005. Allergic conjunctivitis: update on pathophysiology and prospects for future treatment. The Journal of Allergy and Clinical Immunology 115, 118–122.

Peebles Jr., R.S., 2004. Viral infections, atopy, and asthma: is there a causal relationship? The Journal of Allergy and Clinical Immunology 113, S15–S18.

Pinna, A., Zanetti, S., Sotgiu, M., Sechi, L.A., Fadda, G., Carta, F., 1999. Identification and antibiotic susceptibility of coagulase negative staphylococci isolated in corneal/external infections. The British Journal of Ophthalmology 83, 771–773.

Power, W.J., Ghoraishi, M., Merayo-Lloves, J., Neves, R.A., Foster, C.S., 1995. Analysis of the acute ophthalmic manifestations of the erythema multiforme/Stevens-Johnson syndrome/toxic epidermal necrolysis disease spectrum. Ophthalmology 102, 1669–1676.

Prehaud, C., Megret, F., Lafage, M., Lafon, M., 2005. Virus infection switches TLR-3-positive human neurons to become strong producers of beta interferon. J Virol 79, 12893–12904.

Redfern, R.L., Reins, R.Y., McDermott, A.M., 2011. Toll-like receptor activation modulates antimicrobial peptide expression by ocular surface cells. Experimental Eye Research 92, 209–220.

Ritchie, M.D., Hahn, L.W., Roodi, N., Bailey, L.R., Dupont, W.D., Parl, F.F., Moore, J.H., 2001. Multifactor-dimensionality reduction reveals high-order interactions among estrogen-metabolism genes in sporadic breast cancer. Am J Hum Genet 69, 138–147.

Roujeau, J.C., Bracq, C., Huyn, N.T., Chaussalet, E., Raffin, C., Duedari, N., 1986. HLA phenotypes and bullous cutaneous reactions to drugs. Tissue Antigens 28, 251–254.

Roujeau, J.C., Kelly, J.P., Naldi, L., Rzany, B., Stern, R.S., Anderson, T., Auquier, A., Bastuji-Garin, S., Correia, O., Locati, F., et al., 1995. Medication use and the risk of Stevens-Johnson syndrome or toxic epidermal necrolysis. The New England Journal of Medicine 333, 1600–1607.

Saito, H., Kubota, M., Roberts, R.W., Chi, Q., Matsunami, H., 2004. RTP family members induce functional expression of mammalian odorant receptors. Cell 119, 679–691.

Seal, D.V., McGill, J.I., Jacobs, P., Liakos, G.M., Goulding, N.J., 1985. Microbial and immunological investigations of chronic non-ulcerative blepharitis and meibomianitis. The British Journal of Ophthalmology 69, 604–611.

Shaveta, G., Shi, J., Chow, V.T., Song, J., 2010. Structural characterization reveals that viperin is a radical S-adenosyl-L-methionine (SAM) enzyme. Biochemical and Biophysical Research Communications 391, 1390–1395.

Smolin, G., Okumoto, M., 1977. Staphylococcal blepharitis. Archives of Ophthalmology 95, 812–816.

Sotozono, C., Inagaki, K., Fujita, A., Koizumi, N., Sano, Y., Inatomi, T., Kinoshita, S., 2002. Methicillin-resistant *Staphylococcus aureus* and methicillin-resistant *Staphylococcus epidermidis* infections in the cornea. Cornea 21, S94–101.

Sotozono, C., Ang, L.P., Koizumi, N., Higashihara, H., Ueta, M., Inatomi, T., Yokoi, N., Kaido, M., Dogru, M., Shimazaki, J., Tsubota, K., Yamada, M., Kinoshita, S., 2007. New grading system for the evaluation of chronic ocular manifestations in patients with Stevens-Johnson syndrome. Ophthalmology 114, 1294–1302.

Sotozono, C., Ueta, M., Kinoshita, S., 2009a. The management of severe ocular complications of stevens-johnson syndrome and toxic epidermal necrolysis. Archives of Dermatology 145, 1336–1337. author reply 1337–1338.

Sotozono, C., Ueta, M., Koizumi, N., Inatomi, T., Shirakata, Y., Ikezawa, Z., Hashimoto, K., Kinoshita, S., 2009b. Diagnosis and treatment of Stevens-Johnson syndrome and toxic epidermal necrolysis with ocular complications. Ophthalmology 116, 685–690.

Soumelis, V., Reche, P.A., Kanzler, H., Yuan, W., Edward, G., Homey, B., Gilliet, M., Ho, S., Antonenko, S., Lauerma, A., Smith, K., Gorman, D., Zurawski, S., Abrams, J., Menon, S., McClanahan, T., de Waal-Malefyt Rd, R., Bazan, F., Kastelein, R.A., Liu, Y.J., 2002. Human epithelial cells trigger dendritic cell mediated allergic inflammation by producing TSLP. Nature Immunology 3, 673–680.

Stevens, A.M., Johnson, F.C., 1922. A new eruptive fever associated with stomatitis and opthalmia: report of two cases in children. American Journal of Diseases of Children 24, 526–533.

Streilein, J.W., 2003. Ocular immune privilege: therapeutic opportunities from an experiment of nature. Nature Reviews Immunology 3, 879–889.

Strober, W., 2004. Epithelial cells pay a Toll for protection. Nature Medicine 10, 898–900.

Strober, W., Fuss, I.J., Blumberg, R.S., 2002. The immunology of mucosal models of inflammation. Annual Review of Immunology 20, 495–549.

Suzuki, T., Mitsuishi, Y., Sano, Y., Yokoi, N., Kinoshita, S., 2005. Phlyctenular keratitis associated with meibomitis in young patients. American Journal of Ophthalmology 140, 77–82.

Tenover, F.C., Arbeit, R.D., Goering, R.V., Mickelsen, P.A., Murray, B.E., Persing, D.H., Swaminathan, B., 1995. Interpreting chromosomal DNA restriction patterns produced by pulsed-field gel electrophoresis: criteria for bacterial strain typing. Journal of Clinical Microbiology 33, 2233–2239.

Thygeson, P., 1969. Complications of staphylococcic blepharitis. American Journal of Ophthalmology 68, 446–449.

Tokunaga, K., Ishikawa, Y., Ogawa, A., Wang, H., Mitsunaga, S., Moriyama, S., Lin, L., Bannai, M., Watanabe, Y., Kashiwase, K., Tanaka, H., Akaza, T., Tadokoro, K.,

Please cite this article in press as: Ueta, M., Kinoshita, S., Ocular surface inflammation is regulated by innate immunity, Progress in Retinal and Eye Research (2012), http://dx.doi.org/10.1016/j.preteyeres.2012.05.003

Juji, T., 1997. Sequence-based association analysis of HLA class I and II alleles in Japanese supports conservation of common haplotypes. Immunogenetics 46, 199–205.
Ueta, M., 2008. Innate immunity of the ocular surface and ocular surface inflammatory disorders. Cornea 27, S31–S40.
Ueta, M., 2010. Regulation of ocular surface inflammation by prostaglandin E receptor subtype EP3. Cornea 29, S57–S61.
Ueta, M., Kinoshita, S., 2010a. Innate immunity of the ocular surface. Brain Research Bulletin 81, 219–228.
Ueta, M., Kinoshita, S., 2010b. Ocular surface inflammation mediated by innate immunity. Eye & Contact Lens 36, 269–281.
Ueta, M., Nochi, T., Jang, M.H., Park, E.J., Igarashi, O., Hino, A., Kawasaki, S., Shikina, T., Hiroi, T., Kinoshita, S., Kiyono, H., 2004. Intracellularly expressed TLR2s and TLR4s contribution to an immunosilent environment at the ocular mucosal epithelium. The Journal of Immunology 173, 3337–3347.
Ueta, M., Hamuro, J., Kiyono, H., Kinoshita, S., 2005a. Triggering of TLR3 by polyI: C in human corneal epithelial cells to induce inflammatory cytokines. Biochemical and Biophysical Research Communications 331, 285–294.
Ueta, M., Hamuro, J., Yamamoto, M., Kaseda, K., Akira, S., Kinoshita, S., 2005b. Spontaneous ocular surface inflammation and goblet cell disappearance in I kappa B zeta gene-disrupted mice. Investigative Ophthalmology & Visual Science 46, 579–588.
Ueta, M., Iida, T., Sakamoto, M., Sotozono, C., Takahashi, J., Kojima, K., Okada, K., Chen, X., Kinoshita, S., Honda, T., 2007a. Polyclonality of Staphylococcus epidermidis residing on the healthy ocular surface. Journal of Medical Microbiology 56, 77–82.
Ueta, M., Nakamura, T., Tanaka, S., Kojima, K., Kinoshita, S., 2007b. Development of eosinophilic conjunctival inflammation at late-phase reaction in mast cell-deficient mice. The Journal of Allergy and Clinical Immunology 120, 476–478.
Ueta, M., Sotozono, C., Inatomi, T., Kojima, K., Hamuro, J., Kinoshita, S., 2007c. Association of IL4R polymorphisms with stevens-johnson syndrome. The Journal of Allergy and Clinical Immunology 120, 1457–1459.
Ueta, M., Sotozono, C., Inatomi, T., Kojima, K., Tashiro, K., Hamuro, J., Kinoshita, S., 2007d. Toll-like receptor 3 gene polymorphisms in Japanese patients with Stevens-Johnson syndrome. The British Journal of Ophthalmology 91, 962–965.
Ueta, M., Sotozono, C., Tokunaga, K., Yabe, T., Kinoshita, S., 2007e. Strong association between HLA-A*0206 and stevens-johnson syndrome in the Japanese. American Journal of Ophthalmology 143, 367–368.
Ueta, M., Hamuro, J., Ueda, E., Katoh, N., Yamamoto, M., Takeda, K., Akira, S., Kinoshita, S., 2008a. Stat6-independent tissue inflammation occurs selectively on the ocular surface and perioral skin of IkappaBzeta-/- mice. Investigative Ophthalmology & Visual Science 49, 3387–3394.
Ueta, M., Sotozono, C., Inatomi, T., Kojima, K., Hamuro, J., Kinoshita, S., 2008b. Association of combined IL-13/IL-4R signaling pathway gene polymorphism with Stevens-Johnson syndrome accompanied by ocular surface complications. Investigative Ophthalmology & Visual Science 49, 1809–1813.
Ueta, M., Sotozono, C., Inatomi, T., Kojima, K., Hamuro, J., Kinoshita, S., 2008c. Association of Fas ligand gene polymorphism with stevens-johnson syndrome. The British Journal of Ophthalmology 92, 989–991.
Ueta, M., Tokunaga, K., Sotozono, C., Inatomi, T., Yabe, T., Matsushita, M., Mitsuishi, Y., Kinoshita, S., 2008d. HLA class I and II gene polymorphisms in Stevens-Johnson syndrome with ocular complications in Japanese. Molecular Vision 14, 550–555.
Ueta, M., Matsuoka, T., Narumiya, S., Kinoshita, S., 2009a. Prostaglandin E receptor subtype EP3 in conjunctival epithelium regulates late-phase reaction of experimental allergic conjunctivitis. The Journal of Allergy and Clinical Immunology 123, 466–471.
Ueta, M., Sotozono, C., Takahashi, J., Kojima, K., Kinoshita, S., 2009b. Examination of *Staphylococcus aureus* on the ocular surface of patients with catarrhal ulcers. Cornea 28, 780–782.
Ueta, M., Uematsu, S., Akira, S., Kinoshita, S., 2009c. Toll-like receptor 3 enhances late-phase reaction of experimental allergic conjunctivitis. The Journal of Allergy and Clinical Immunology 123, 1187–1189.
Ueta, M., Hamuro, J., Kinoshita, S., 2010a. Spatio-temporal dual effects of IkappaB-zeta dictates the caution on visual disturbance resulting from IkappaBzeta deficiency. Immunology Letters 133, 115.
Ueta, M., Mizushima, K., Yokoi, N., Naito, Y., Kinoshita, S., 2010b. Gene-expression analysis of polyI: C-stimulated primary human conjunctival epithelial cells. The British Journal of Ophthalmology 94, 1528–1532.
Ueta, M., Sotozono, C., Nakano, M., Taniguchi, T., Yagi, T., Tokuda, Y., Fuwa, M., Inatomi, T., Yokoi, N., Tashiro, K., Kinoshita, S., 2010c. Association between prostaglandin E receptor 3 polymorphisms and Stevens-Johnson syndrome identified by means of a genome-wide association study. The Journal of Allergy and Clinical Immunology 126, 1218–1225. e1210.
Ueta, M., Kawai, T., Yokoi, N., Akira, S., Kinoshita, S., 2011a. Contribution of IPS-1 to polyI: C-induced cytokine production in conjunctival epithelial cells. Biochemical and Biophysical Research Communications 404, 419–423.
Ueta, M., Matsuoka, T., Yokoi, N., Kinoshita, S., 2011b. Prostaglandin E2 suppresses polyinosine-polycytidylic acid (polyI: C)-stimulated cytokine production via prostaglandin E2 receptor (EP) 2 and 3 in human conjunctival epithelial cells. The British Journal of Ophthalmology 95, 859–863.
Ueta, M., Matsuoka, T., Yokoi, N., Kinoshita, S., 2011c. Prostaglandin E receptor subtype EP3 downregulates TSLP expression in human conjunctival epithelium. The British Journal of Ophthalmology 95, 742–743.
Ueta, M., Sotozono, C., Yokoi, N., Inatomi, T., Kinoshita, S., 2011d. Prostaglandin E receptor subtype EP3 expression in human conjunctival epithelium and its changes in various ocular surface disorders. PloS One 6, e25209.
Ueta, M., Sotozono, C., Yokoi, N., Kinoshita, S., 2012a. Downregulation of monocyte chemoattractant protein 1 expression by prostaglandin E(2) in human ocular surface epithelium. Archives of Ophthalmology 130, 249–251.
Ueta, M., Tamiya, G., Tokunaga, K., Sotozono, C., Ueki, M., Sawai, H., Inatomi, T., Matsuoka, T., Akira, S., Narumiya, S., Tashiro, K., Kinoshita, S., 2012b. Epistatic interaction between Toll-like receptor 3 (TLR3) and prostaglandin E receptor 3 (PTGER3) genes. The Journal of Allergy and Clinical Immunology 129, 1413–1416.
Vane, J.R., Bakhle, Y.S., Botting, R.M., 1998. Cyclooxygenases 1 and 2. Annual Review of Pharmacology and Toxicology 38, 97–120.
Wolf, R., Orion, E., Marcos, B., Matz, H., 2005. Life-threatening acute adverse cutaneous drug reactions. Clinics in Dermatology 23, 171–181.
Xu, Y., Johansson, M., Karlsson, A., 2008. Human UMP-CMP kinase 2, a novel nucleoside monophosphate kinase localized in mitochondria. The Journal of Biological Chemistry 283, 1563–1571.
Yamamoto, M., Yamazaki, S., Uematsu, S., Sato, S., Hemmi, H., Hoshino, K., Kaisho, T., Kuwata, H., Takeuchi, O., Takeshige, K., Saitoh, T., Yamaoka, S., Yamamoto, N., Yamamoto, S., Muta, T., Takeda, K., Akira, S., 2004. Regulation of Toll/IL-1-receptor-mediated gene expression by the inducible nuclear protein IkappaB-zeta. Nature 430, 218–222.
Yamane, Y., Aihara, M., Ikezawa, Z., 2007. Analysis of Stevens-Johnson syndrome and toxic epidermal necrolysis in Japan from 2000 to 2006. Allergology International 56, 419–425.
Yamazaki, S., Muta, T., Takeshige, K., 2001. A novel IkappaB protein, IkappaB-zeta, induced by proinflammatory stimuli, negatively regulates nuclear factor-kappaB in the nuclei. The Journal of Biological Chemistry 276, 27657–27662.
Yetiv, J.Z., Bianchine, J.R., Owen Jr., J.A., 1980. Etiologic factors of the stevens-johnson syndrome. Southern Medical Journal 73, 599–602.
Ying, S., O'Connor, B., Ratoff, J., Meng, Q., Mallett, K., Cousins, D., Robinson, D., Zhang, G., Zhao, J., Lee, T.H., Corrigan, C., 2005. Thymic stromal lymphopoietin expression is increased in asthmatic airways and correlates with expression of Th2-attracting chemokines and disease severity. The Journal of Immunology 174, 8183–8190.
Ying, S., O'Connor, B., Ratoff, J., Meng, Q., Fang, C., Cousins, D., Zhang, G., Gu, S., Gao, Z., Shamji, B., Edwards, M.J., Lee, T.H., Corrigan, C.J., 2008. Expression and cellular provenance of thymic stromal lymphopoietin and chemokines in patients with severe asthma and chronic obstructive pulmonary disease. The Journal of Immunology 181, 2790–2798.
Zhang, J., Xu, K., Ambati, B., Yu, F.S., 2003. Toll-like receptor 5-mediated corneal epithelial inflammatory responses to Pseudomonas aeruginosa flagellin. Investigative ophthalmology & visual science 44, 4247–4254.
Zhang, D., Zhang, G., Hayden, M.S., Greenblatt, M.B., Bussey, C., Flavell, R.A., Ghosh, S., 2004. A toll-like receptor that prevents infection by uropathogenic bacteria. Science 303, 1522–1526.
Zhang, J., Kumar, A., Wheater, M., Yu, F.S., 2008. Lack of MD-2 expression in human corneal epithelial cells is an underlying mechanism of lipopolysaccharide (LPS) unresponsiveness. Immunology and Cell Biology 87, 141–148.
Ziegler, S.F., Liu, Y.J., 2006. Thymic stromal lymphopoietin in normal and pathogenic T cell development and function. Nature Immunology 7, 709–714.

Abbreviation

PFGE: pulsed-field gel electrophoresis
TLRs: Toll-like receptors
IFN: interferon
IL: interleukin
TNF: tumor necrosis factor
PGN: peptidoglycan
ds: double-stranded
polyI:C: polyinosine-polycytidylic acid
LPS: Lipopolysaccharide
CpG: deoxy-cytidylate-phosphate-deoxy-guanylate
RT-PCR: reverse transcription-polymerase chain reaction
IP-10: IFN-gamma inducible protein 10
NLRs: nucleotide-binding oligomerization domain (NOD)-like receptors
RLRs: retinoic acid-inducible gene-I (RIG-I)-like receptors
Mx2: myxovirus (influenza virus) resistance 2
Rsad2: radical S-adenosyl methionine domain containing 2
Cmpk2: cytidine monophosphate (UMP-CMP) kinase 2
Cxcl10: chemokine (C-X-C motif) ligand 10
Mx1: myxovirus (influenza virus) resistance 1
Ifi44: interferon-induced protein 44
Ifi203: interferon-activated gene 203
Iigp2: interferon-inducible GTPase 2
Rtp4: receptor transporter protein 4
TSLP: thymic stromal lymphopoietin
PG: prostaglandin
TX: thromboxane
SJS: Stevens-Johnson syndrome
TEN: toxic epidermal necrolysis
NSAIDs: non-steroidal anti-inflammatory drugs

Please cite this article in press as: Ueta, M., Kinoshita, S., Ocular surface inflammation is regulated by innate immunity, Progress in Retinal and Eye Research (2012), http://dx.doi.org/10.1016/j.preteyeres.2012.05.003

The American Journal of Pathology, Vol. 181, No. 1, July 2012

http://dx.doi.org/10.1016/j.ajpath.2012.03.033

Stem Cells, Tissue Engineering, and Hematopoietic Elements

ROCK Inhibitor Converts Corneal Endothelial Cells into a Phenotype Capable of Regenerating *In Vivo* Endothelial Tissue

Naoki Okumura,*† Noriko Koizumi,† Morio Ueno,* Yuji Sakamoto,† Hiroaki Takahashi,† Hideaki Tsuchiya,‡ Junji Hamuro,* and Shigeru Kinoshita*

From the Department of Ophthalmology, Kyoto Prefectural University of Medicine, Kyoto; the Department of Biomedical Engineering,† Faculty of Life and Medical Sciences, Doshisha University, Kyotanabe; and the Research Center for Animal Life Science,‡ Shiga University of Medical Science, Otsu, Japan*

Corneal endothelial dysfunction accompanied by visual disturbance is a primary indication for corneal transplantation. We previously reported that the adhesion of corneal endothelial cells (CECs) to a substrate was enhanced by the selective ROCK inhibitor Y-27632. It is hypothesized that the inhibition of ROCK signaling may manipulate cell adhesion properties, thus enabling the transplantation of cultivated CECs as a form of regenerative medicine. In the present study, using a rabbit corneal endothelial dysfunction model, the transplantation of CECs in combination with Y-27632 successfully achieved the recovery of corneal transparency. Complications related to cell injection therapy, such as the abnormal deposition of the injected cells as well as the elevation of intraocular pressure, were not observed. Reconstructed corneal endothelium with Y-27632 exhibited a monolayer hexagonal cell shape with a normal expression of function-related markers, such as ZO-1, and Na^+/K^+-ATPase, whereas reconstruction without Y-27632 exhibited a stratified fibroblastic phenotype without the expression of markers. Moreover, transplantation of CECs in primates in the presence of the ROCK inhibitor also achieved the recovery of long-term corneal transparency with a monolayer hexagonal cell phenotype at a high cell density. Taken together, these results suggest that the selective ROCK inhibitor Y-27632 enables cultivated CEC-based therapy and that the modulation of Rho-ROCK signaling activity serves to enhance cell engraftment for cell-based regenerative medicine. *(Am J Pathol 2012, 181:268–277; http://dx.doi.org/10.1016/j.ajpath.2012.03.033)*

Corneal endothelial dysfunction is a major cause of severe visual impairment, because corneal endothelial cells maintain corneal transparency through their barrier and Na^+-K^+ transport system. Highly effective surgical techniques to replace corneal endothelium (eg, Descemet's stripping endothelial keratoplasty) have been developed,[1,2] aimed at replacing penetrating keratoplasty for overcoming pathological dysfunctions of corneal endothelial tissue. Several research groups, including ours, have devoted an intensive amount of effort in an attempt to establish new treatment methods suitable for a practical clinical intervention to repair corneal endothelial dysfunctions.[3–6] Because corneal endothelium is composed of a monolayer and is technically difficult to transplant into the anterior chamber as a structurally flexible cell sheet, those research teams cultured corneal endothelial cells (CECs) on substrates such as collagen sheets and amniotic membrane.

The injection of cultivated cells has been reported for the treatment of a number of organs associated with degenerative diseases such as the heart,[7] vessels,[8] pancreas,[9] and cartilage.[10] In regard to corneal endothelium, it is known that injected cultured CECs appear to be washed off by aqueous humor flow, thus resulting in the poor adhesion of those injected cells onto the corneal tissue. To develop an effective method for delivering cultivated CECs to the posterior cornea, the magnetic attachment of iron powder or superparamagnetic microspheres incorporated in the cultivated CECs has been attempted. This method has been shown to work in a

Supported in part by the Highway Program for realization of regenerative medicine (S.K. and N.O.) and the Funding Program for Next Generation World-Leading Researchers from the Cabinet Office in Japan (LS117 to N.K.).

Accepted for publication March 27, 2012.

Address reprint requests to Noriko Koizumi, M.D., Ph.D., Department of Biomedical Engineering, Faculty of Life and Medical Sciences, Doshisha University, Kyotanabe 610-0321, Japan. E-mail: nkoizumi@mail.doshisha.ac.jp.

rabbit transplantation model[11,12] and in an organ culture model of the human eye[13]; however, these methods have yet to be applied in the clinical setting.

Cell adhesion is known to be mediated through transmembrane adhesion molecules linked to the intracellular cytoskeleton. In addition to the structural function, these adhesion molecules reportedly serve as a platform for the interplay with the surrounding environments.[14,15] Rho GTPase proteins are key modulators of cytoskeletal dynamics that occur after cell adhesion.[16–18] It has been reported that Rho GTPases induce a specific type of actin cytoskeleton through mediating downstream effectors mDia and Rho-associated kinase (ROCK), and that they regulate a variety of cellular functions.[19] Cell adhesion, motility, and cell morphogenesis are thought to be determined by the balance between mDia and ROCK activities.[19] We recently reported that the adhesion of CECs to a substrate was enhanced by inhibiting Rho/ROCK signaling.[20] This finding coincides well with those of other studies that demonstrated that Rho-ROCK signaling negatively regulates the integrin-mediated adhesion of monocytes, and that the inhibition of ROCK by a selective ROCK inhibitor upregulates adhesion.[17,18] These features have led us to hypothesize that the inhibition of ROCK signaling may provide a way to manipulate the cell adhesion property of cultivated corneal endothelium to the extent practical for regenerative medicine.

In this current study, in two animal models (rabbit and primate) of corneal endothelial dysfunctions, the transplantation of cultivated CECs in combination with ROCK inhibitor Y-27632 successfully achieved the recovery of corneal transparency. Inhibition of the ROCK signaling manipulated the adhesion property of the cultivated CECs. Moreover, the injected CECs functioned sufficiently well to reconstruct the corneal endothelium with an appropriate cell density, morphology, and expression of function-related markers. This novel treatment strategy may provide a new therapeutic modality for corneal-endothelium–associated pathological dysfunctions.

Materials and Methods

Materials

Rabbit eyes were purchased from Funakoshi Corporation (Tokyo, Japan). Alizarin red S stain and selective ROCK inhibitor Y-27632 were purchased from Wako Pure Chemical Industries, Ltd. (Osaka, Japan). Dulbecco's modified Eagle's medium supplemented with penicillin, streptomycin, and basic fibroblast growth factor (bFGF), Vybrant DiI cell-labeling solution, Alexa Fluor 594-conjugated phalloidin, Alexa Fluor 488-conjugated phalloidin, Alexa Fluor 488-conjugated goat anti-mouse IgG, anti-vinculin antibody, ROCK1 Stealth RNAi (HSS109291, HSS109292, and HSS109293), ROCK2 Stealth RNAi (HSS114106, HSS114107, and HSS114108), Stealth RNAi negative control medium GC #2, and Lipofectamine RNAiMAX were purchased from Life Technologies (Carlsbad, CA). Dispase II was purchased from Roche Applied Science (Penzberg, Germany). FNC Coating Mix was purchased from Athena Environmental Sciences, Inc. (Baltimore, MD). Ki-67 monoclonal antibody, propidium iodide (PI), and Cytochalasin D were purchased from Sigma-Aldrich Co. (St. Louis, MO). ZO-1 polyclonal antibody was purchased from Zymed Laboratories (South San Francisco, CA). α–Smooth muscle actin (α-SMA) monoclonal antibody was purchased from Thermo Fisher Scientific (Kalamazoo, MI). Na^+/K^+-ATPase monoclonal antibody was purchased from Upstate Biotech (Lake Placid, NY). DAPI was purchased from Vector Laboratories (Burlingame, CA). CellTiter-Glo Luminescent Cell Viability Assay was purchased from Promega (Madison, WI).

Animal Experiment Approval

In all experiments, animals were housed and treated in accordance with The Association for Research in Vision and Ophthalmology Statement for the Use of Animals in Ophthalmic and Vision Research. The rabbit experiments were performed at Doshisha University (Kyoto, Japan) according to the protocol approved by that university's Animal Care and Use Committee (approval no. 0831). The monkey experiments were performed at the Research Center for Animal Life Science at Shiga University of Medical Science (Otsu, Japan) according to the protocol approved by that university's Animal Care and Use Committee (approval no. 2008-10-5).

Cell Culture of Rabbit and Monkey CECs

Ten rabbit eyes were used for the rabbit CECs (RCECs) culture. Eight corneas from four cynomolgus monkeys (3 to 5 years of age; estimated equivalent human age: 5 to 20 years) housed at the Nissei Bilis Co. (Otsu, Japan) and the Keari Co. (Wakayama, Japan), respectively, were used for the monkey CECs (MCECs) culture. The RCECs and MCECs were cultivated as described previously.[3,20] Briefly, Descemet's membrane with CECs was stripped and incubated in 0.6 U/mL of Dispase II to release the CECs. After a 60-minute incubation at 37°C, the CECs obtained from individual corneas were resuspended in culture medium and plated in one well of a six-well plate coated with cell attachment reagent (FNC Coating Mix). All primary cell cultures and serial passages of CECs were performed in growth medium composed of Dulbecco's modified Eagle's medium supplemented with 10% fetal bovine serum, 50 U/mL penicillin, 50 μg/mL streptomycin, and 2 ng/mL bFGF. CECs were cultured in a humidified atmosphere at 37°C in 5% CO_2. The culture medium was changed every 2 days. When cells reached confluency in 10 to 14 days, they were rinsed in Ca^{2+} and Mg^{2+}-free Dulbecco's phosphate-buffered saline (PBS), trypsinized with 0.05% Trypsin-EDTA (Life Technologies, Carlsbad, CA) for 5 minutes at 37°C, and passaged at ratios of 1:2 to 1:4. Cultivated CECs derived from both rabbit and monkey corneas at passages 3 through 5 were used for all experiments. To confirm the cultivation of the CECs, the morphology and density of the cultivated cells were compared with normal *in vivo* rabbit CECs examined using a noncontact specular microscope (Noncon Robo, SP-8800; Konan Medical, Nishinomiya,

Japan) and stained with Alizarin red. In some experiments, to investigate the fate of the injected CECs *in vivo*, the CECs were labeled with fluorescein by use of the Vybrant DiI cell-labeling solution according to the manufacturer's protocol.

Rabbit Corneal Endothelial Dysfunction Model

To create rabbit corneal endothelial pathological dysfunction models, the lenses of both eyes of 12 Japanese white rabbits were removed under general anesthesia by use of the Alcon Series 20000 Legacy Surgical System (Alcon, Fort Worth, TX) to deepen the anterior chamber. Next, the corneal endothelium of each of those eyes was mechanically scraped with a 20-gauge silicone needle (Soft Tapered Needle; Inami, Tokyo, Japan) from Descemet's membrane as described previously.[3,4] The scraped area was then confirmed by 0.04% trypan blue staining during surgery. In the preliminary experiments, we confirmed that Descemet's membrane was intact, the mechanically scraped area had no cells on Descemet's membrane, and that residual CECs were detected in only a 500- to 600-μm area at the edge of Descemet's membrane.

Injection of Cultivated CECs into the Rabbit Eyes

To evaluate the injection of cultivated CECs with ROCK inhibitor, RCECs at a density of 2.0×10^5 cells were suspended in 200 μl DMEM supplemented with 100 μmol/L of Y-27632 and then injected into the anterior chamber of the eyes of the above-described corneal endothelial dysfunction rabbit model. RCECs with Y-27632 were injected into the right eyes of six rabbits, and RCECs without Y-27632 were injected into the right eyes of the other six rabbits. After the injection, the eyes of those 12 rabbits were kept in the face-down position for 3 hours under general anesthesia. The left eyes of those 12 rabbits in which the corneal endothelium was removed mechanically were used as a control. One rabbit injected with RCECs with Y-27632 and one rabbit injected with RCECs without Y-27632 were euthanized 3 hours after injection for histological examination. The corneal appearance of the other 10 rabbits was examined daily by use of a slit-lamp microscope for the first week, and then once every 2 days for the following 2 weeks. Those 10 rabbits were then euthanized for histological examination. Corneal thickness was determined by use of an ultrasound pachymeter (SP-2000; Tomey, Nagoya, Japan), and the mean of 10 measured values was then calculated (up to a maximum thickness of 1200 μm, the instrument's maximum reading). Intraocular pressure was measured by use of a pneumatonometer (30 Classic; Reichert, NY).

Histological Examination of Rabbit Eyes After CEC Injection

Sections (6-μm) of corneal specimens obtained from the 10 rabbits euthanized 2 weeks after injection were embedded in OCT compound and then fixed in 4% formaldehyde. Differential interference contrast (DIC) images and fluorescence images of DiI-labeled cells were obtained by use of a fluorescence microscope (TCS SP2 AOBS; Leica Microsystems, Welzlar, Germany). For flat-mount examinations, whole corneal specimens were fixed in 4% formaldehyde and incubated in 1% bovine serum albumin (BSA) to block any nonspecific binding. To evaluate the effect of Y-27632 on the adhesion property of the cells, corneas obtained from the 2 rabbits euthanized 3 hours after injection were examined by actin staining performed with a 1:400 dilution of Alexa Fluor 488–conjugated phalloidin. Actin staining was used to evaluate the cellular morphology. The cell nuclei were then stained with PI. To investigate the phenotype of the reconstructed corneal endothelium obtained from the 10 rabbits euthanized 2 weeks after injection, immunohistochemical analyses of actin, α-SMA, ZO-1, Na^+/K^+-ATPase, DiI, and Ki-67 were performed. α-SMA was used to evaluate the fibroblastic change. ZO-1, a tight-junction–associated protein, and Na^+/K^+-ATPase, the protein associated with pump function, were used for function related markers of CECs. The α-SMA, ZO-1, and Na^+/K^+-ATPase staining were performed with a 1:200 dilution of α-SMA monoclonal antibody, ZO-1 polyclonal antibody, and Na^+/K^+-ATPase monoclonal antibody, respectively. Ki-67 (a cell-proliferation–related maker) staining was performed using a 1:400 dilution of anti-mouse Ki-67 antibody. For the secondary antibody, a 1:2000 dilution of Alexa Fluor 488–conjugated goat anti-mouse IgG was used. Cell nuclei were then stained with DAPI, and the slides were inspected by fluorescence microscopy.

Effect of Y-27632 on MCECs in Culture

MCECs were cultured at a density of 2.5×10^4 cells/cm^2 on Lab-Tek Chamber Slides (NUNC A/S, Roskilde, Denmark). Actin staining was performed with 1:400-diluted Alexa Fluor, as described above, after 24 hours of seeding, and vinculin staining was performed using 1:200-diluted vinculin after 3 hours of seeding. The number of attached MCECs was evaluated by use of CellTiter-Glo Luminescent Cell Viability Assay performed according to the manufacturer's protocol. The MCECs were seeded with a different concentration of Y-27632 at the density of 1.0×10^3 cells onto 96-well plates, and the number of adhered MCECs at 24 hours after seeding was then measured by use of a Veritas Microplate Luminometer (Promega). In addition to ROCK signaling inhibition, to evaluate the effect of inhibition of actin polymerization on CECs adhesion, MCECs were seeded with a different concentration of cytochalasin D at the density of 1.0×10^3 cells onto 96-well plates, and the number of adhered MCECs at 24 hours after seeding was then measured. Five samples were prepared for each group.

To determine the adhesion property of the MCECs onto the basement membrane, the cells were seeded onto rabbit corneas in which the corneal endothelium was mechanically denuded and the basement membranes were exposed. The cells were seeded at the density of 2.5×10^4 cells/cm^2 suspended in culture medium supplemented with or without 10 μmol/L Y-27632. Actin staining was performed at 3 hours after seeding in the same

manner as with the Alexa Fluor 488–conjugated phalloidin staining described above. Cell nuclei were then stained with PI. MCECs at the density of 2.0×10^5 cells were also seeded, with or without Y-27632, onto Descemet's membrane of four rabbits from each group, and the membrane was then mechanically peeled off at 3 hours after seeding. The adhered MCECs were recovered by trypsin digestion, and the cell numbers were then counted.

Inhibition of ROCK Signaling by siRNA on MCECs in Culture

MCECs seeded at the density of 2.5×10^4 cells/cm^2 onto a 24-well plate were incubated with RNAi duplex (ROCK1 Stealth RNAi and ROCK2 Stealth RNAi) and Lipofectamine RNAiMAX according to the manufacturer's protocol. Briefly, 1 day before transfection, the culture medium was replaced with fresh medium without antibiotics. RNAi duplex at the final concentration of 10 nmol/L and Lipofectamine RNAiMAX complexes were added to each well. The MCECs were incubated for 12 hours at 37°C in a CO_2 incubator. Random RNAi was used as a control. The MCECs were then seeded at the density of 1.0×10^3 cells onto 96-well plates, and the number of attached MCECs was evaluated by use of CellTiter-Glo Luminescent Cell Viability Assay. Knockdown of both ROCK1 and ROCK2, two ROCK isoforms that were identified in the mammalian system,[21] was confirmed by quantitative PCR analysis (data not shown). Representative data were from six independent experiments using three kinds of ROCK1 Stealth RNAi and ROCK2 Stealth RNAi, respectively.

Injection of Cultivated CECs into Monkey Eyes with Corneal Endothelial Dysfunction

To create monkey corneal endothelial pathological dysfunction models, the corneal endothelium of the left eyes of four monkeys was mechanically scraped with a 20-gauge silicone needle under general anesthesia, as described above for the rabbit model. Next, a 2.0×10^5 density of cultivated MCECs suspended in 200 μl DMEM supplemented with 100 μmol/L Y-27632 were injected into the anterior chamber of two of the four monkeys. Cultivated MCECs suspended in 200 μl DMEM without Y-27632 were injected into the anterior chamber of the other 2 monkeys. The eyes of all four monkeys were kept in the face-down position for 3 hours under general anesthesia. The MCECs were labeled with DiI before transplantation.[3,4] The corneal appearance of all four monkeys was examined daily by use of a slit-lamp microscope for the first week, and then once per week for the following 3 months. Two monkeys from each group (the MCEC-injection with Y-27632 group, and the MCEC-injection without Y-27632 group) were euthanized at 14 days after the injection, and the other 2 monkeys were euthanized at 3 months after the injection. For flat-mount examinations, whole corneal specimens were fixed in 4% formaldehyde, incubated in 1% BSA to block nonspecific binding, and then prepared for histological examination. To investigate the phenotype of the reconstructed corneal endothelium, immunohistochemical analyses of actin, ZO-1, and Na^+/K^+-ATPase were performed in the same manner as that of the above-described rabbit experiments. After the actin immunostaining, the corneal endothelium of the four monkeys was evaluated by KSS-400EB software version 2.71 (Konan Medical, Hyogo, Japan).

Statistical Analysis

The statistical significance (P value) in mean values of the two-sample comparison was determined by Student's t-test. Values shown on the graphs represent the mean ± SEM.

Results

Injection of Cultivated RCECs with ROCK Inhibitor Enables Regeneration of Cornea in Rabbit Corneal Endothelial Dysfunction Model

The third-passaged RCECs exhibited a monolayer of hexagonal shaped cells, similar to *in vivo* RCECs with a cell density of approximately 2600 cells/mm^2 as previously reported[5,6] (Figure 1A). Cultivated RCECs injected together with Y-27632 were successful in recovering complete transparency of the corneas with pathological dysfunctions. In contrast, RCECs injected without Y-27632 induced hazy and severely edematous corneas, thus indicating that the corneal endothelial dysfunctions were sustained, comparable with those of the control corneas. Slit-lamp microscopy performed at 48 hours after injection revealed complete corneal transparency with the iris and the pupil clearly observed in the eyes injected with RCECs with Y-27632, whereas the iris and pupil could not be observed in the eyes injected with RCECs without Y-27632 and in the control eyes in which the corneal endothelium was mechanically scraped (Figure 1B). Consistent with the slit-lamp microscopy findings, histological analysis performed at 14 days after injection also revealed that the eyes injected with RCECs with Y-27632 had a normal range of corneal thickness, whereas those without Y-27632 exhibited a thick cornea with severe stromal edema. The corneal thicknesses of those specimens were 409 μm and 730 μm, respectively (Figure 1C). In the eyes injected with RCECs with Y-27632, the corneal edema was moderate (<800 μm) at day 1, yet gradually recovered to the normal level. In contrast, in both the control eyes and the eyes injected with RCECs without Y-27632, prominent corneal edema (>1200 μm) was observed at day 1, and corneal edema persisted throughout the observation period (Figure 1D). Next, possible complications associated with cell injection into the anterior chamber were investigated, as the injected cells might possibly interfere with normal aqueous humor outflow and produce an increase in intraocular pressure. No abnormal deposition of the injected DiI-positive RCECs onto the trabecular meshwork or onto the iris and no anatomical abnormality such as mechanical angle closure or peripheral anterior synechia were de-

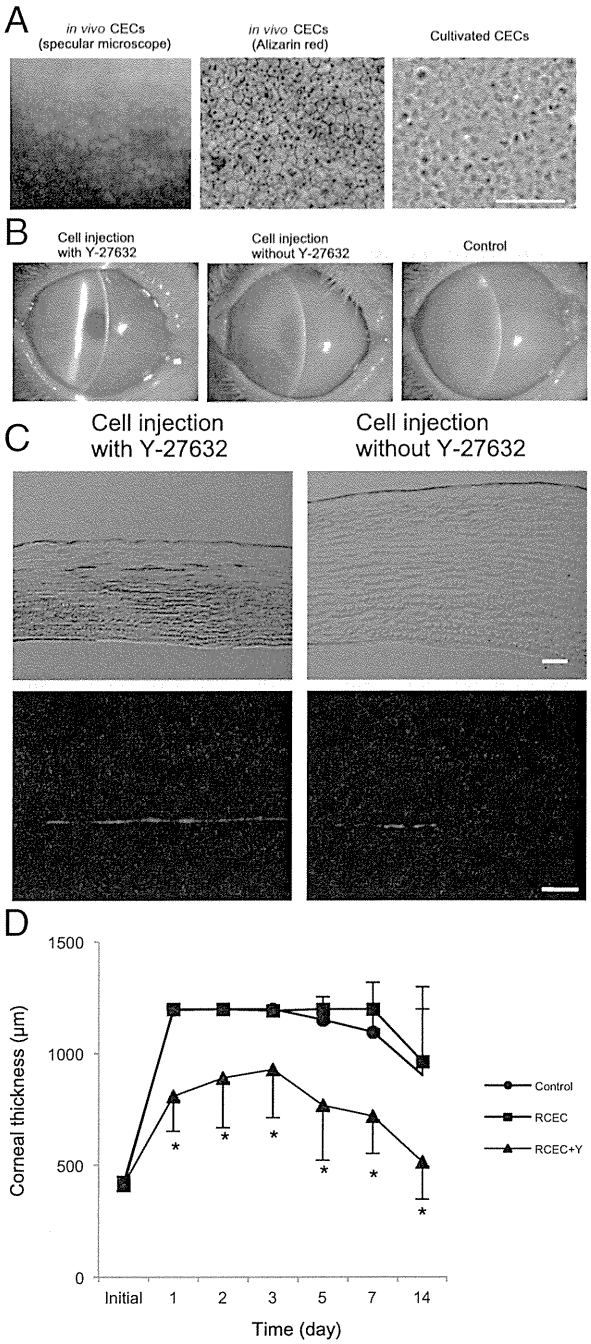

Figure 1. Cell regeneration in a rabbit corneal endothelial dysfunction model. **A:** *In vivo* normal corneal endothelium (**left panel:** specular microscope, **middle panel:** Alizarin red staining) and cultivated rabbit corneal endothelial cells (RCECs) (**right panel:** phase contrast image). The cultivated RCECs exhibit a homogeneous monolayer of hexagonal cells with a cell density of approximately 2600 cells/mm^2. The morphology and density of the cultivated RCECs are similar to that of *in vivo* corneal endothelium. Scale bar = 100 μm. **B:** Slit-lamp photographs of rabbit eyes injected with cultivated RCECs with Y-27632, cultivated RCECs without Y-27632, and control corneal endothelial dysfunction model after 48 hours. **C:** Histological analysis of rabbit corneas injected with cultivated RCECs with (**left column**) or without (**right column**) Y-27632 (**top row:** DIC; **bottom row:** DiI). Injection of RCECs with Y-27632 induces a normal-range thickness (409 μm) of the cornea, whereas injection of RCECs without Y-27632 exhibits a thick (730 μm) cornea with severe corneal stromal edema at 14 days after injection. Scale bars: 100 μm. **D:** Time course of corneal thickness measured by ultrasound pachymeter. In control eyes and in the eyes injected with RCECs without Y-27632, the corneal edema is prominent (>1200 μm) at day 1 and persists throughout the observation period. In contrast, in the eyes injected with RCECs with Y-27632, the corneal edema is moderate (<800 μm) at day 1 and gradually recovers to the normal level.

tected (Figure 2A). Intraocular pressures were found to be in the normal range in all groups (Figure 2B). To evaluate the injected CECs proliferation status *in vivo*, a flat-mount cornea was examined at 14 days after injection. Immunofluorescence analysis using the Ki-67 monoclonal antibody (a marker of cell proliferation) revealed that the cell cycle of the nearly all of the injected cells was arrested 2 weeks after injection (Figure 2C). These results

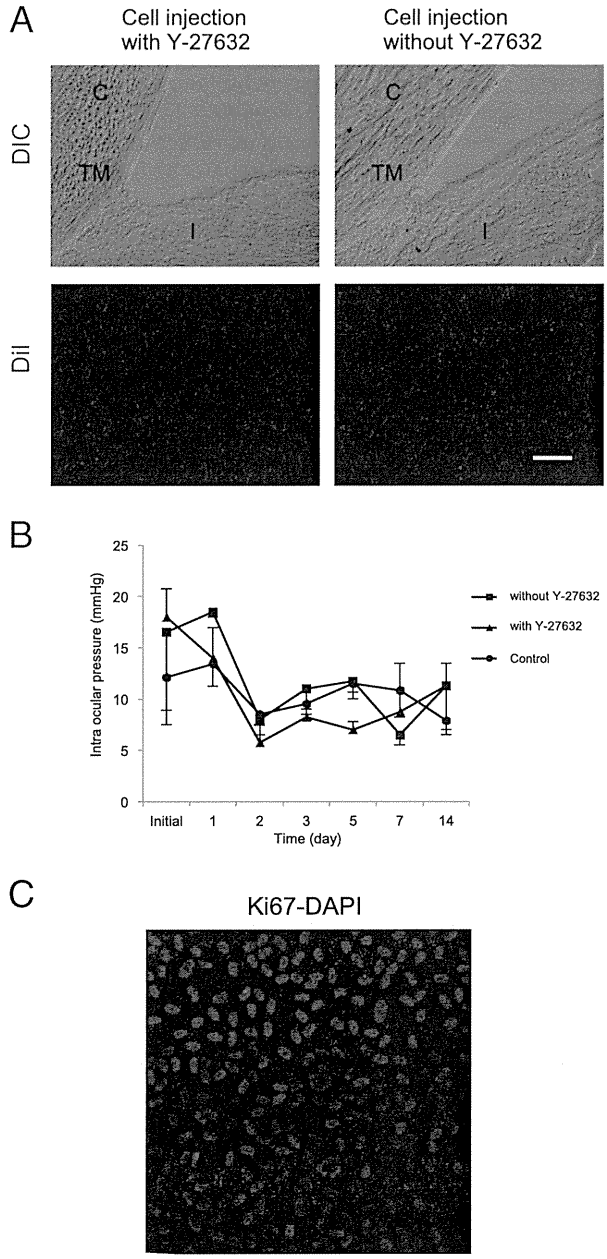

Figure 2. Evaluation of the possible adverse effects of cultivated RCEC injection. **A:** Histological examination of the iris and the angle tissue. **Top row:** representative images of the DIC section taken from the rabbit eye injected with cultivated RCECs with or without Y-27632 after 14 days. **Bottom row:** DiI images of the same sections shown in the **top row**. C, cornea; I, iris; TM, trabecular meshwork. Scale bar = 100 μm. **B:** Intraocular pressures after the injection of RCECs. **C:** Immunohistochemical staining for cell proliferation marker Ki-67 in the reconstructed RCECs in the eye injected with RCECs with Y-27632 on day 14.

indicate that ROCK inhibitor can be safely applied for cell injection therapy.

ROCK Inhibitor Provides RCECs with Phenotype to Reconstruct Corneal Endothelium

At 3 hours after injection, RCECs injected with Y-27632 were found to be markedly adhered to the basement membrane of the corneal endothelium (Figure 3A), suggesting that Y-27632 altered the adhesion properties of the RCECs and up-regulated cell adhesion on the basement membrane *in vivo*. To ascertain the causal effect of the elevated cell adhesion by Y-27632 in the induction of a pathologically transparent cornea, the histological phenotype of a donor cornea treated with Y-27632 was elucidated using a flat-mount cornea. The expression of ZO-1 and Na^+/K^+-ATPase was evident in RCECs injected with Y-27632, yet it was absent in RCECs injected without Y-27632. RCECs injected with Y-27632 exhibited a monolayer hexagonal cell shape, whereas RCECs injected without Y-27632 exhibited the stratified fibroblastic phenotype. Consistent with the stratified fibroblastic phenotype of RCECs injected without Y-27632, α-SMA (a marker of fibroblastic change) was evident in those RCECs (Figure 3B).

The existence of reconstructed corneal endothelium by the injection of RCECs with Y-27632 that expressed DiI, which labels RCECs, indicated that the injected RCECs contributed to the formation of a monolayer of corneal endothelium and to the inducement of corneal transparency (Figure 3B). However, DiI-expressing cells were also observed in the rabbits injected with RCECs without Y-27632, consistent with the results shown in Figure 1C. The presence of DiI-positive cells in the eyes injected with RCECs without Y-27632 may suggest that a limited number of RCECs were able to adhere to the cornea without the assistance of Y-27632, yet changed their phenotype to that of fibroblastic cells. This finding is consistent with those observed in the clinical setting, in which CECs display a fibroblastic phenotype in cases of corneal endothelial dysfunction.[22,23]

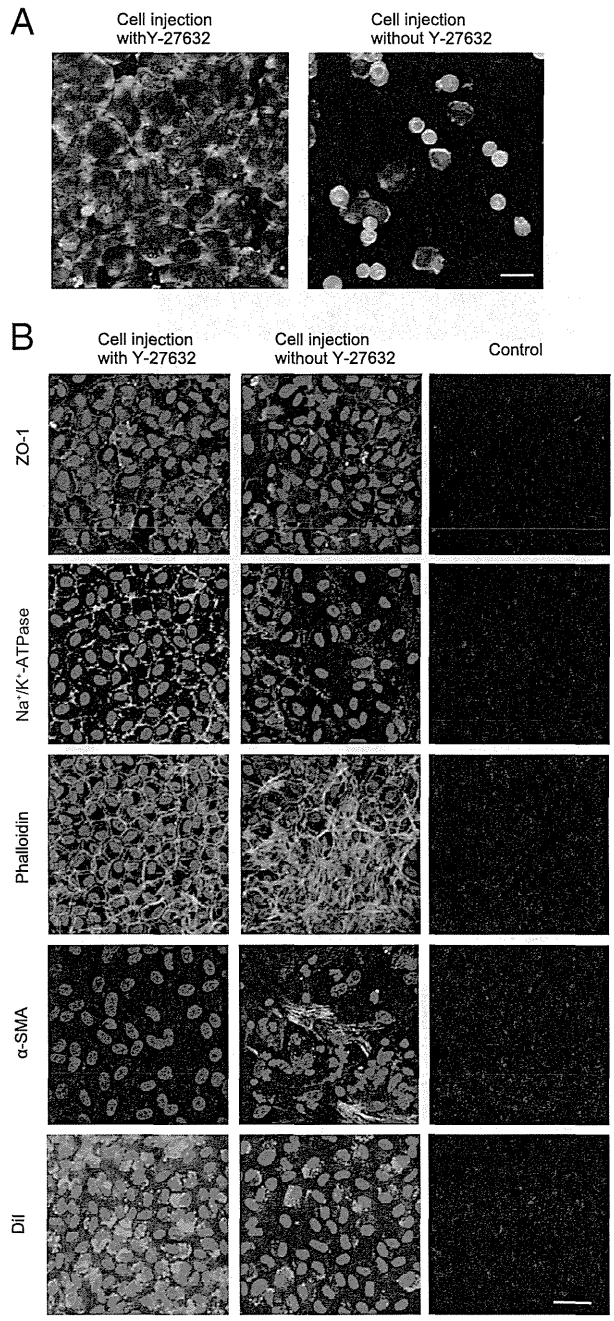

Figure 3. Histological examination of the reconstructed corneal tissue in rabbits after RCEC injection with and without Y-27632. **A:** Flat-mount examination of the posterior side of the corneal tissue 3 hours after RCEC injection. Green fluorescein shows actin-staining (phalloidin), and red shows nuclear staining by propidium iodide (PI). Scale bar = 100 μm. **B:** Histological examination of corneal tissue taken from the rabbit eye 2 weeks after RCEC injection with or without Y-27632. The histological phenotype of the injected RCECs was evaluated by immunofluorescence of ZO-1, Na^+/K^+-ATPase, phalloidin, α-SMA, and DiI after 2 weeks. No cells are observed in the control eyes in which the corneal endothelium was scraped. Scale bar = 100 μm.

ROCK Inhibitor Y-27632 Enhances Cell Adhesion

To examine the role of the Rho/ROCK signaling pathway in modulating the adhesion properties of primate CECs, cultivated MCECs were plated in combination with ROCK inhibitor Y-27632. Consistent with our previous findings,[20] phase contrast imaging and actin fiber staining revealed elevated cell adhesion in the Y-27632 treated cells (Figure 4A), and the cell adhesion was enhanced at the conventionally used concentration[24] (Figure 4B). MCECs treated with Y-27632 showed a markedly improved expression of vinculin in contrast to the non-treated cells (Figure 4C), suggesting that Y-27632 enhanced the cell adhesion via the induction of focal adhesion complexes. Considering the interplay between focal adhesion complex molecules and the extracellular matrix,[15] we next attempted to clarify the effect of Y-27632 on MCEC adhesion onto Descemet's membrane (basement membrane). Consistent with the *in vivo* experiments shown in Figure 3A, an *ex vivo* culture system

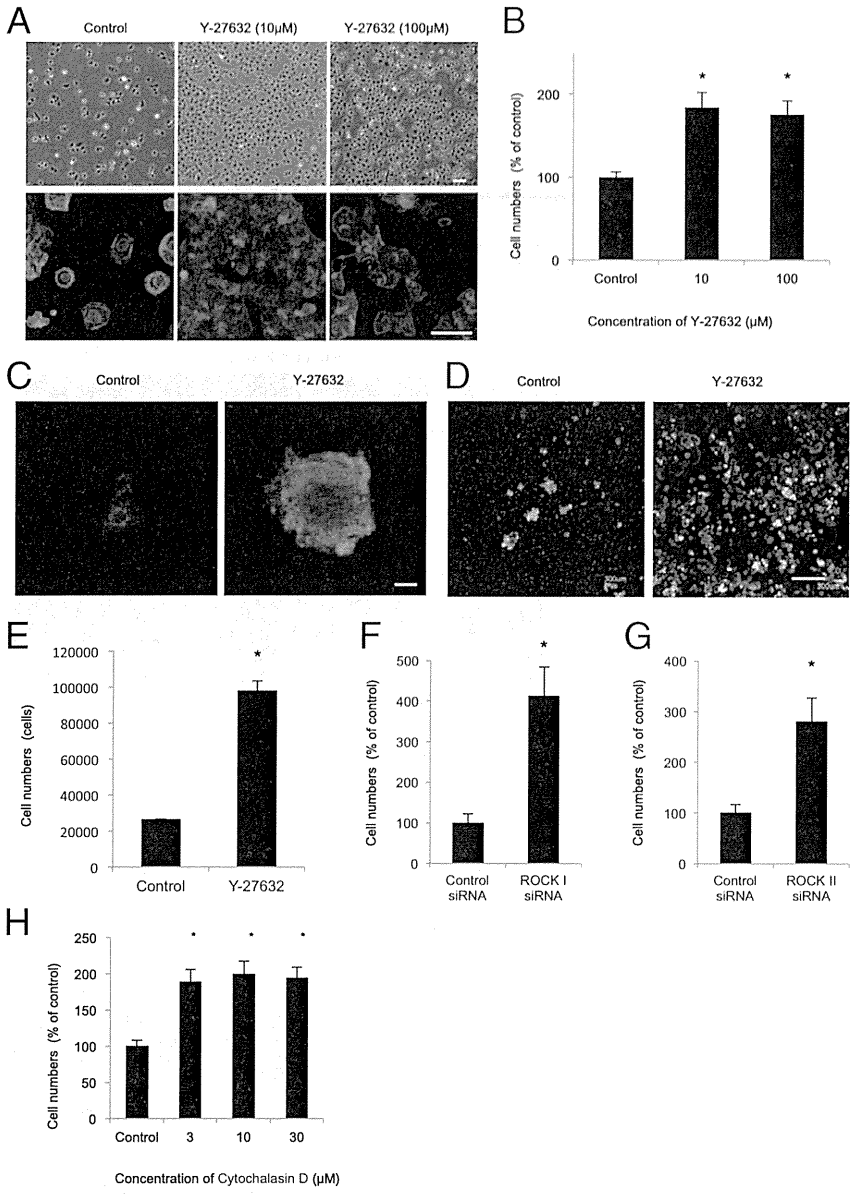

Figure 4. Rho/ROCK signaling pathway modulation of the adhesion properties of primate CECs in culture. **A:** Phase contrast images (**top row**) and actin fiber staining images (**bottom row**) reveal elevated cell adhesion in Y-27632–treated monkey CECs (MCECs) at 24 hours after seeding on a culture dish. Scale bar = 100 μm (**top row**), 50 μm (**bottom row**). **B:** The number of adhered MCECs is significantly enhanced by 10 μmol/L and 100 μmol/L of Y-27632 at 24 hours after seeding. Data are expressed as a percentage of the control, mean ± SEM. $^*P < 0.01$. **C:** Representative immunofluorescence images of MCECs seeded with or without Y-27632 taken after staining with anti-vinculin at 3 hours after seeding. Scale bar = 10 μm. **D:** MCECs were seeded with or without Y-27632 on *ex vivo* culture system of rabbit Descemet's membrane and stained with actin antibody at 3 hours after seeding. Green fluorescein shows actin staining (phalloidin), and red shows nuclear staining by propidium iodide (PI). Scale bar = 300 μm. **E:** MCECs (density: 2.0×10^5 cells) were seeded with or without Y-27632 on rabbit Descemet's membrane, and the number of adhered cells was evaluated at 3 hours after seeding. Data are expressed as mean ± SEM. $^*P < 0.01$. **F** and **G:** Direct contribution of the Rho/ROCK signaling pathway to the regulation of the adhesion properties of CECs was assessed by the knockdown of ROCK1 (**F**) or ROCK2 (**G**). Results are expressed as a percentage of the control, mean ± SEM. $^*P < 0.01$. **H:** MCEC attachment was assessed through the inhibition of actin polymerization by cytochalasin D. Results are expressed as a percentage of the control, mean ± SEM. $^*P < 0.01$.

demonstrated that Y-27632 dramatically enhanced the adhesion of the MCECs onto the basement membrane at 3 hours after seeding (Figure 4, D and E).

The direct contribution of the Rho/ROCK signaling pathway in elevating the adhesion properties was elucidated by the knockdown of ROCK I and ROCK II by RNAi (Figure 4, F and G; confirmed with three independent RNAi). Coincidentally, as with the elevated cell adhesion by Y-27632, the knockdown of both ROCK I and ROCK II strongly enhanced the cell adhesion. Because ROCK signaling is necessary to negatively regulate cell adhesion by inhibiting actin depolymerization, we speculate that inhibition of ROCK by Y-27632 promotes actin reorganization, subsequently inducing the enhancement of cell adhesion. In accordance with that speculation, we found that cytochalasin D, which is additionally capable of inhibiting actin polymerization, also elevated the MCEC adhesion (Figure 4H).

Injection of Cultivated CECs with ROCK Inhibitor Enables Regeneration of Cornea in a Primate Model

The injection of cultivated MCECs combined with Y-27632 was performed in a cynomolgus monkey in which the corneal endothelium was mechanically removed to produce a pathological dysfunction model. To elucidate the long-term efficacy of the injection of CECs with ROCK inhibitor Y-27632, that monkey model was observed for 3 months. In contrast to the rabbit model, slit-lamp microscopy showed that the monkey eyes injected with MCECs, both with and without Y-27632, exhibited complete corneal transparency within 1 week, and that the transparency persisted throughout 3 months of cell injection with a normal range of thickness (<600 μm) (Figure 5A). To evaluate the histological phenotype of donor corneas, two of four mon-

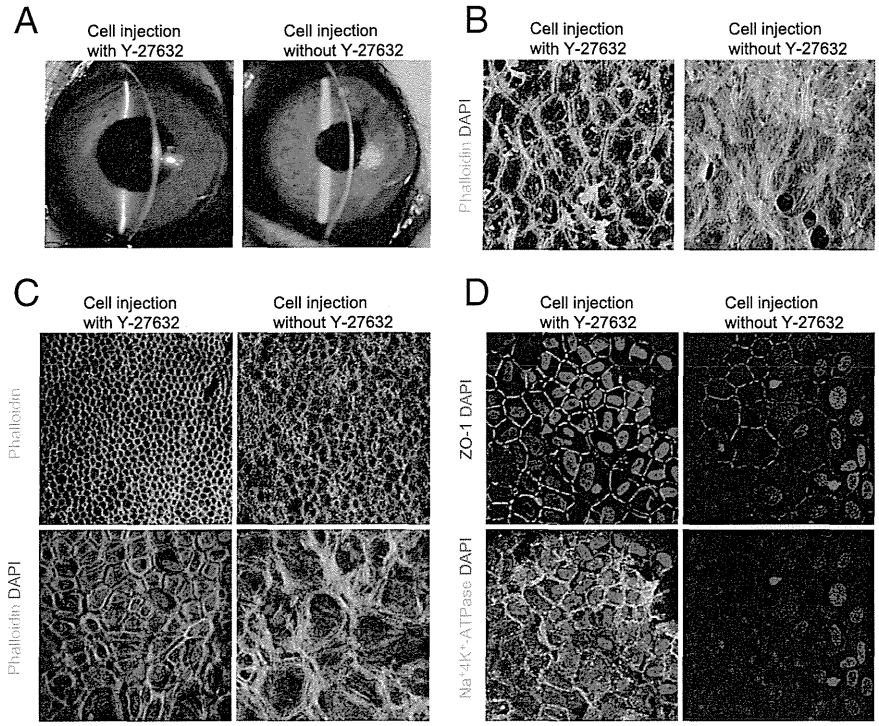

Figure 5. Regeneration of the cornea in a primate model enabled by the injection of cultivated MCECs with Y-27632. **A:** Monkey eyes injected with MCECs with Y-27632 or without Y-27632 exhibit a transparent cornea with a normal range of thickness (<600 μm) after 3 months. **B:** Histological analysis by actin immunostaining after 2 weeks of cell injection of MCECs injected with or without Y-27632. **C:** Histological analysis by actin immunostaining after 3 months of cell injection of MCECs injected with or without Y-27632. **Top row:** lower magnification (green, actin); **bottom row:** higher magnification (green, actin; blue, DAPI). The cell density of the MCECs injected without Y-27632 was 789 cells/mm^2, whereas that with Y-27632 was 2208 cells/mm^2. **D:** Histological analysis was performed after immunostaining of ZO-1 (red) or Na^+/K^+-ATPase (green). DAPI was used for nuclei staining (blue).

keys were euthanized after 2 weeks of MCEC injection and the other two monkeys after 3 months of MCEC injection (one monkey that received MCEC injection with Y-27632 and one monkey that received MCEC injection without Y-27632, respectively, at each of the two time points). It is notable that the MCECs injected with Y-27632 exhibited a monolayer cell shape, whereas the MCECs injected without Y-27632 exhibited a stratified fibroblastic phenotype at the 2-week time point, which mirrored the rabbit model findings (Figure 5B). Although slit-lamp microscopy showed that the monkey eyes injected with MCECs, both with and without Y-27632, exhibited a transparent cornea with a normal-range corneal thickness, MCECs injected without Y-27632 exhibited a fibroblastic phenotype at the cell density of 789 cells/mm^2, whereas MCECs injected with Y-27632 exhibited a monolayer hexagonal cell phenotype at the cell density of 2208 cells/mm^2 (Figure 5C), suggesting that Y-27632 also enhanced the adhesion of MCECs in the *in vivo* monkey model. Consistent with the rabbit experiments, the MCECs injected with Y-27632 expressed ZO-1 and Na^+/K^+-ATPase, yet they were expressed to a lesser degree in the MCECs injected without Y-27632 that exhibited the fibroblastic phenotype (Figure 5D).

Discussion

Corneal endothelial dysfunction accompanied by visual disturbance is a major indication for corneal transplantation surgery.[25] Although corneal transplantation is widely performed for corneal endothelial dysfunction, the transplantation of cultivated corneal endothelium is a potential therapeutic strategy. Cultivated CECs derived from older donors have lower proliferative ability, a senescent cell phenotype, and transformed cell morphology, thus suggesting less functional ability than those derived from younger donors.[26] When corneal endothelium is cultured and stocked as "master cells," it allows for the transplantation of CECs derived from younger donors, thus providing cells with high functional ability and an extended longevity. In addition, it enables an HLA-matching transplantation to reduce the risk of rejection[27,28] and to overcome the shortage of donor corneas. In the clinical setting, transplantation of corneal endothelium is technically difficult, because it is a monolayer and is located in the anterior chamber. Thus, that anatomical feature led us to hypothesize that the injection of cultivated CECs would be a potent therapy, even though a previous study reported that cell injection itself was ineffective.[12] The findings of this present study show that the inclusion of ROCK inhibitor Y-27632 elevates the adhesion property of CECs, thus allowing the successful transplantation of CECs to reconstruct functional corneal endothelium damaged by pathological dysfunctions.

We previously reported that the inhibition of ROCK by use of the selective ROCK inhibitor Y-27632 elevates the adhesion of cultured CECs on the substrate, enhances cell proliferation, and suppresses apoptosis.[20] Although the precise underlying mechanisms have yet to be elucidated, those distinct positive effects of ROCK inhibition enable the establishment of the *in vitro* expansion of CECs for cultivated corneal endothelial transplantation.[20] Rho–ROCK signaling carries out a variety of cellular processes such as cell adhesion, morphogenesis, migration, and cell-cycle progression through mediating cytoskeletal dynamics. The Rho GTPase-specific guanine nucleotide exchange factors (Rho GEFs) convert Rho from the guanosine diphosphate (GDP)–bound inactive form to

the guanosine triphosphate (GTP)–bound active form, thus inducing Rho GTPase activity. Rho regulates a variety of cytoskeletal dynamics that underlie cell morphology and adhesion through the activation of ROCK, a major downstream effector.[16,19] ROCK signaling modulates acto-myosin contractility through the regulation of myosin phosphorylation and actin dynamics by promoting nucleation and polymerization or by stimulating the severing and depolymerization of existing actin filaments.[17,29] It is reported that the actin cytoskeleton plays a critical role in regulating the adhesive property through interaction between the actin cytoskeleton and integrin.[14,17,18] Although the adhesive property is dependent on the cell type and the environmental context, ROCK signaling has been shown to negatively regulate the integrin adhesions of monocytes[17] and leukocytes.[18] Findings from a recent study showed that the RhoA–ROCK–PTEN pathway was highly activated when pre-osteoblasts are poorly attached to the substrate, and that the inhibition of this pathway enhances cell adhesion as well as proliferation.[30] Our findings that the inhibition of ROCK signaling by a selective ROCK inhibitor or by the siRNA enhanced adhesive property of CECs are consistent with the findings of those previous studies. Our findings are also supported by our data that inhibiting actin polymerization by cytochalasin D enhances the adhesive property. Furthermore, we found that vinculin, which is involved in the linkage of the integrin adhesion complex to the actin cytoskeleton,[31,32] is upregulated in ROCK-inhibitor-treated CECs. Further investigation is needed to elucidate whether the ROCK inhibitor promotes the focal adhesions through inhibiting actin polymerization and induces the upregulation of cell adhesion properties on the extracellular matrix (ECM).

Corneal endothelial dysfunctions such as Fuchs's endothelial corneal dystrophy, pseudoexfoliation syndrome, keratitis, and injury induce the fibroblastic transformation of CECs.[22,23] In addition, CECs reportedly showed fibroblastic transformation during the wound healing process,[33] and IL-1β–mediated FGF-2 produced after an injury reportedly alters CEC morphology and the actin cytoskeleton in a rabbit freezing injury model.[34] Our findings that RCECs without Y-27632 injected into the anterior chamber of a bullous keratopathy rabbit model exhibited stratified fibroblastic cell morphology and a resultant opaque cornea are consistent with these studies. On the other hand, MCECs without Y-27632 exhibited less fibroblastic phenotype. In our current primate model, a low density of MCECs compensated the pump and barrier functions and resulted in a clear cornea. That finding might possibly be explained by differences in the wound healing process between species.[35,36] However, because CEC density continuously decreases after keratoplasty,[37] reconstructed corneal endothelium with Y-27632 at a high cell density is crucial for the successful long-term outcome of transplantation in the clinical setting. To establish the application of a cultivated CEC injection combined with ROCK inhibitor in clinical settings, transplantation models more akin to humans are required, as rabbit CECs exhibit a high proliferative ability *in vivo*,[38] unlike human CECs. The findings from this present study demonstrated that a monkey eye injected with MCECs with Y-27632 exhibited an almost completely clear cornea. Thus, our primate model–based findings suggest that the cell injection therapy in which the cell adhesion is modulated by ROCK inhibitor might prove to be an effective treatment regimen for human corneal endothelial disorders.

In regard to future clinical applications, ROCK inhibitors have been shown to be useful for a wide range of diseases such as cardiovascular disease, pulmonary disease, cancer, and glaucoma.[21,39–41] Fasudil, one of the ROCK inhibitors, has already been used clinically for the prevention and treatment of cerebral vasospasm, and to date has been therapeutically applied in over 124,000 cases in Japan.[21] Furthermore, we previously demonstrated that a ROCK inhibitor eye drop enhanced corneal endothelial proliferation *in vitro*,[20] as well as in an *in vivo* animal model,[42] and it is currently under clinical research for corneal endothelial dysfunction. These facts suggest that the ROCK inhibitor is a therapeutic tool that can be safely and effectively applied in the clinical setting.

In conclusion, the findings of this present study, which are supported by both rabbit and primate corneal endothelial dysfunction models, indicate that ROCK inhibitor Y-27632 will enable the establishment of a cultivated-CEC–based therapy. Modulating actin cytoskeletal dynamics through Rho-ROCK signaling activity serves as a potential for cell-based regenerative medicine to enhance cell engraftment. This novel strategy of using a cell-based therapy combined with a ROCK inhibitor may ultimately provide clinicians with a new therapeutic modality in regenerative medicine, not only for the treatment of corneal endothelial dysfunctions but also for a variety of pathological diseases.

Acknowledgments

We thank Drs. Yoshiki Sasai and Masatoshi Ohgushi for assistance and invaluable advice regarding ROCK inhibitors, Takahiro Nakagawa for assistance with the monkey experiments, Kenta Yamasaki, Mayumi Yamamoto, Yuri Tsukahara, and Toshie Isobe for technical assistance, and John Bush for reviewing the manuscript.

References

1. Gorovoy MS: Descemet-stripping automated endothelial keratoplasty. Cornea 2006, 25:886–889
2. Price FW, Jr., Price MO: Descemet's stripping with endothelial keratoplasty in 50 eyes: a refractive neutral corneal transplant. J Refract Surg 2005, 21:339–345
3. Koizumi N, Sakamoto Y, Okumura N, Okahara N, Tsuchiya H, Torii R, Cooper LJ, Ban Y, Tanioka H, Kinoshita S: Cultivated corneal endothelial cell sheet transplantation in a primate model. Invest Ophthalmol Vis Sci 2007, 48:4519–4526
4. Koizumi N, Sakamoto Y, Okumura N, Tsuchiya H, Torii R, Cooper LJ, Ban Y, Tanioka H, Kinoshita S: Cultivated corneal endothelial transplantation in a primate: possible future clinical application in corneal endothelial regenerative medicine. Cornea 2008, 27 Suppl 1:S48–S55
5. Mimura T, Yamagami S, Yokoo S, Usui T, Tanaka K, Hattori S, Irie S, Miyata K, Araie M, Amano S: Cultured human corneal endothelial cell

transplantation with a collagen sheet in a rabbit model. Invest Ophthalmol Vis Sci 2004, 45:2992–2997
6. Ishino Y, Sano Y, Nakamura T, Connon CJ, Rigby H, Fullwood NJ, Kinoshita S: Amniotic membrane as a carrier for cultivated human corneal endothelial cell transplantation. Invest Ophthalmol Vis Sci 2004, 45:800–806
7. Schachinger V, Erbs S, Elsasser A, Haberbosch W, Hambrecht R, Holschermann H, Yu J, Corti R, Mathey DG, Hamm CW, Suselbeck T, Assmus B, Tonn T, Dimmeler S, Zeiher AM: Intracoronary bone marrow-derived progenitor cells in acute myocardial infarction. N Engl J Med 2006, 355:1210–1221
8. Tateishi-Yuyama E, Matsubara H, Murohara T, Ikeda U, Shintani S, Masaki H, Amano K, Kishimoto Y, Yoshimoto K, Akashi H, Shimada K, Iwasaka T, Imaizumi T: Therapeutic angiogenesis for patients with limb ischaemia by autologous transplantation of bone-marrow cells: a pilot study and a randomised controlled trial. Lancet 2002, 360:427–435
9. Shapiro AM, Lakey JR, Ryan EA, Korbutt GS, Toth E, Warnock GL, Kneteman NM, Rajotte RV: Islet transplantation in seven patients with type 1 diabetes mellitus using a glucocorticoid-free immunosuppressive regimen. N Engl J Med 2000, 343:230–238
10. Yanaga H, Koga M, Imai K, Yanaga K: Clinical application of biotechnically cultured autologous chondrocytes as novel graft material for nasal augmentation. Aesthetic Plast Surg 2004, 28:212–221
11. Mimura T, Shimomura N, Usui T, Noda Y, Kaji Y, Yamgami S, Amano S, Miyata K, Araie M: Magnetic attraction of iron-endocytosed corneal endothelial cells to Descemet's membrane. Exp Eye Res 2003, 76: 745–751
12. Mimura T, Yamagami S, Usui T, Ishii Y, Ono K, Yokoo S, Funatsu H, Araie M, Amano S: Long-term outcome of iron-endocytosing cultured corneal endothelial cell transplantation with magnetic attraction. Exp Eye Res 2005, 80:149–157
13. Patel SV, Bachman LA, Hann CR, Bahler CK, Fautsch MP: Human corneal endothelial cell transplantation in a human ex vivo model. Invest Ophthalmol Vis Sci 2009, 50:2123–2131
14. Sastry SK, Burridge K: Focal adhesions: a nexus for intracellular signaling and cytoskeletal dynamics. Exp Cell Res 2000, 261:25–36
15. Critchley DR: Focal adhesions—the cytoskeletal connection. Curr Opin Cell Biol 2000, 12:133–139
16. Hall A: Rho GTPases and the actin cytoskeleton. Science 1998, 279:509–514
17. Worthylake RA, Lemoine S, Watson JM, Burridge K: RhoA is required for monocyte tail retraction during transendothelial migration. J Cell Biol 2001, 154:147–160
18. Worthylake RA, Burridge K: RhoA and ROCK promote migration by limiting membrane protrusions. J Biol Chem 2003, 278:13578–13584
19. Narumiya S, Tanji M, Ishizaki T: Rho signaling, ROCK and mDia1, in transformation, metastasis and invasion. Cancer Metastasis Rev 2009, 28:65–76
20. Okumura N, Ueno M, Koizumi N, Sakamoto Y, Hirata K, Hamuro J, Kinoshita S: Enhancement on primate corneal endothelial cell survival in vitro by a ROCK inhibitor. Invest Ophthalmol Vis Sci 2009, 50: 3680–3687
21. Liao JK, Seto M, Noma K: Rho kinase (ROCK) inhibitors. J Cardiovasc Pharmacol 2007, 50:17–24
22. Naumann GO, Schlotzer-Schrehardt U: Keratopathy in pseudoexfoliation syndrome as a cause of corneal endothelial decompensation: a clinicopathologic study. Ophthalmology 2000, 107:1111–1124
23. Kawaguchi R, Saika S, Wakayama M, Ooshima A, Ohnishi Y, Yabe H: Extracellular matrix components in a case of retrocorneal membrane associated with syphilitic interstitial keratitis. Cornea 2001, 20:100–103
24. Narumiya S, Ishizaki T, Uehata M: Use and properties of ROCK-specific inhibitor Y-27632. Methods Enzymol 2000, 325:273–284
25. Darlington JK, Adrean SD, Schwab IR: Trends of penetrating keratoplasty in the United States from 1980 to 2004. Ophthalmology 2006, 113:2171–2175
26. Joyce NC, Zhu CC: Human corneal endothelial cell proliferation: potential for use in regenerative medicine. Cornea 2004, 23:S8–S19
27. Khaireddin R, Wachtlin J, Hopfenmuller W, Hoffmann F: HLA-A. HLA-B and HLA-DR matching reduces the rate of corneal allograft rejection. Graefes Arch Clin Exp Ophthalmol 2003, 241:1020–1028
28. Coster DJ, Williams KA: The impact of corneal allograft rejection on the long-term outcome of corneal transplantation. Am J Ophthalmol 2005, 140:1112–1122
29. Ishizaki T, Uehata M, Tamechika I, Keel J, Nonomura K, Maekawa M, Narumiya S: Pharmacological properties of Y-27632, a specific inhibitor of rho-associated kinases. Mol Pharmacol 2000, 57:976–983
30. Yang S, Kim HM: The RhoA-ROCK-PTEN pathway as a molecular switch for anchorage dependent cell behavior. Biomaterials 2012, 33:2902–2915
31. Geiger B: A 130K protein from chicken gizzard: its localization at the termini of microfilament bundles in cultured chicken cells. Cell 1979, 18:193–205
32. Burridge K, Feramisco JR: Microinjection and localization of a 130K protein in living fibroblasts: a relationship to actin and fibronectin. Cell 1980, 19:587–595
33. Ichijima H, Petroll WM, Jester JV, Barry PA, Andrews PM, Dai M, Cavanagh HD: In vivo confocal microscopic studies of endothelial wound healing in rabbit cornea. Cornea 1993, 12:369–378
34. Lee HT, Lee JG, Na M, Kay EP: FGF-2 induced by interleukin-1 beta through the action of phosphatidylinositol 3-kinase mediates endothelial mesenchymal transformation in corneal endothelial cells. J Biol Chem 2004, 279:32325–32332
35. Matsubara M, Tanishima T: Wound-healing of the corneal endothelium in the monkey: a morphometric study. Jpn J Ophthalmol 1982, 26:264–273
36. Matsubara M, Tanishima T: Wound-healing of corneal endothelium in monkey: an autoradiographic study. Jpn J Ophthalmol 1983, 27:444–450
37. Bourne WM, Nelson LR, Hodge DO: Central corneal endothelial cell changes over a ten-year period. Invest Ophthalmol Vis Sci 1997, 38:779–782
38. Van Horn DL, Sendele DD, Seideman S, Buco PJ: Regenerative capacity of the corneal endothelium in rabbit and cat. Invest Ophthalmol Vis Sci 1977, 16:597–613
39. Koga T, Awai M, Tsutsui J, Yue BY, Tanihara H: Rho-associated protein kinase inhibitor, Y-27632, induces alterations in adhesion, contraction and motility in cultured human trabecular meshwork cells. Exp Eye Res 2006, 82:362–370
40. Olson MF: Applications for ROCK kinase inhibition. Curr Opin Cell Biol 2008, 20:242–248
41. Tokushige H, Inatani M, Nemoto S, Sakaki H, Katayama K, Uehata M, Tanihara H: Effects of topical administration of y-39983, a selective rho-associated protein kinase inhibitor, on ocular tissues in rabbits and monkeys. Invest Ophthalmol Vis Sci 2007, 48:3216–3222
42. Okumura N, Koizumi N, Ueno M, Sakamoto Y, Takahashi H, Hirata K, Torii R, Hamuro J, Kinoshita S: Enhancement of corneal endothelium wound healing by Rho-associated kinase (ROCK) inhibitor eye drops. Br J Ophthalmol 2011, 95:1006–1009

Simultaneous Analysis of Multiple Cytokines in the Vitreous of Patients with Sarcoid Uveitis

Kenji Nagata,[1] *Kazuichi Maruyama,*[1] *Kazuko Uno,*[2] *Katsuhiko Shinomiya,*[1] *Kazuhito Yoneda,*[1] *Junji Hamuro,*[1] *Sunao Sugita,*[3] *Takeru Yoshimura,*[4] *Koh-Hei Sonoda,*[5] *Manabu Mochizuki,*[3] *and Shigeru Kinoshita*[1]

Purpose. Levels of some cytokines are significantly higher in the vitreous fluid of patients with acute uveitis than in normal vitreous fluid. The authors sought to determine which proinflammatory cytokines were upregulated in the vitreous fluid of patients with ocular sarcoidosis.

Methods. Samples of vitreous fluid were collected from patients with sarcoid uveitis and from nonsarcoid control patients with idiopathic epiretinal membrane. The levels of 27 proinflammatory cytokines were measured with a multiplex beads array system. Postvitrectomy macular thickness was also measured by using spectral domain optical coherence tomography (SD-OCT). To assess the relationship between cytokine levels and disease stage, the authors divided patients into three groups based on macular thickness 1 month after operation.

Results. The vitreous levels of 17 cytokines were significantly higher in patients with ocular sarcoidosis than in nonsarcoid controls. Serum levels of interferon γ-induced protein 10 (IP-10) were also higher in ocular sarcoidosis patients than in nonsarcoid controls. Conversely, serum levels of interleukin (IL) 15 in ocular sarcoidosis patients were lower than in the control group. Analysis of cytokine levels and macular thickness revealed that IL-1ra, IL-4, IL-8, IFN-γ, IP-10, monocyte chemotactic protein (MCP)-1, macrophage inflammatory protein (MIP)-1β, and regulated on activation, normal T-cell expressed and secreted (RANTES) were significantly upregulated in patients with thin cystoid macular edema group.

Conclusions. Patients with ocular sarcoidosis had elevated levels of proinflammatory cytokines in vitreous fluids. Different cytokines might contribute to different stages of macular edema. (*Invest Ophthalmol Vis Sci.* 2012;53:3827–3833) DOI: 10.1167/iovs.11-9244

From the [1]Department of Ophthalmology, Kyoto Prefectural University of Medicine, Kyoto, Japan; the [2]Louis Pasteur Center for Medical Research, Kyoto, Japan; the [3]Department of Ophthalmology, Tokyo Dental and Medical University, Tokyo, Japan; the [4]Department of Ophthalmology, Graduate School of Medical Science, Kyushu University, Fukuoka, Japan; and the [5]Department of Ophthalmology, Yamaguchi University Graduate School of Medicine, Yamaguchi, Japan.

Supported by KAKEN 22791679 and KAKEN 10433244.

Submitted for publication December 5, 2011; revised March 30 and April 28, 2012; accepted May 4, 2012.

Disclosure: **K. Nagata**, None; **K. Maruyama**, None; **K. Uno**, None; **K. Shinomiya**, None; **K. Yoneda**, None; **J. Hamuro**, None; **S. Sugita**, None; **T. Yoshimura**, None; **K.-H. Sonoda**, None; **M. Mochizuki**, None; **S. Kinoshita**, None

Corresponding author: Kazuichi Maruyama, Department of Ophthalmology, Kyoto Prefectural University of Medicine, 465 Kajii-cho, Hirokoji-agaru, Kawaramachi-dori, Kamigyo-ku, Kyoto 602-0841, Japan; kmaruyam@koto.kpu-m.ac.jp.

Sarcoidosis is a chronic multisystem granulomatous disorder of unknown etiology.[1–4] It is thought to result from an exaggerated cellular immune response to a variety of self-antigens or nonself antigens.[5] The lung is the organ most frequently affected by this disease, and when affected, it is characterized by bilateral hilar lymphadenopathy and/or pulmonary infiltration as revealed by chest radiography. Ocular and skin lesions are also common aspects of sarcoidosis, but other organs (including the heart, the central nervous system, and the spleen) may also be affected.[6] Although the exact cause of sarcoidosis is currently unknown, previous reports have discussed environmental (e.g., spatial[7] or climatic[8]) factors, occupational factors, or infectious agents (specifically, propionibacteria[9–11]) as possible causes.

Reportedly, 30% to 60% of patients with sarcoidosis suffer from ocular involvement.[12–15] Bilateral anterior and/or posterior uveitis is common, but the conjunctiva, lacrimal gland, and orbit of the eye can also be affected. The clinical presentation of sarcoidosis-related uveitis is characteristically marked by iris nodules, mutton-fat keratic precipitates, and tent-shaped peripheral anterior synechia in the anterior segment of the eye. Snowball-like vitreous opacity, which results from phlebitis and vitreitis, is a common posterior segment finding. Chronic uveitis can result in formation of an epiretinal membrane (ERM) and cystoid macular edema (CME); consequently, severe visual impairment can occur.[16] Uveitis is commonly treated with topical (or occasionally systemic) administration of corticosteroids, but in cases accompanied by the formation of an ERM or long-standing vitreous opacity, surgical treatment is necessary.

An internationally acknowledged set of criteria for the diagnosis of ocular sarcoidosis has been established.[17] Previously, it has been reported that the types of cytokines in ocular fluids are dependent on the disease.[18,19] The authors thus sought to assess vitreous cytokine levels and correlate them with disease status in ocular sarcoidosis. The multiplex bead analysis system is a new technique that combines the principle of the sandwich immunoassay with fluorescent bead-based technology. Levels of many types of cytokines in small sample volumes (such as vitreous samples) can be measured simultaneously with this system. Sato et al.[20] have used this method to show that the levels of vascular endothelial growth factor A (VEGF-A) are much higher than those of any type of cytokine in infants with retinopathy of prematurity (ROP). There are also several reports about the levels of various cytokines in vitreous fluid from uveitis patients.[21–25] Yoshimura et al.[18] reported that interleukin (IL) 6, IL-8, and monocyte chemotactic protein-1 (MCP-1) were elevated in the vitreous body of patients with diabetic retinopathy and retinal vein occlusion.

Analyses of many cytokines in peripheral blood or bronchoalveolar lavage fluid (BALF) have elucidated the

pathogenesis of sarcoidosis. For example, high amounts of interferon γ-induced protein 10 (IP-10) are secreted from sarcoid-dependent alveolar macrophages and T cells.[26] However, to the authors' knowledge, investigations of cytokine levels in both vitreous fluid and serum from patients with sarcoid uveitis have not been conducted with multiplex bead analysis.

Here, the vitreous and serum levels of 27 types of cytokines in patients with sarcoid uveitis were measured and compared with those from patients with idiopathic ERM. Moreover, the authors investigated the relationship between vitreous cytokine levels and CME severity.

Methods

Patients

This study was performed in accordance with the tenets of the Declaration of Helsinki, and the procedures were approved by the Institutional Review Board of the Kyoto Prefectural University of Medicine Hospital. Twenty-one patients gave informed consent for participation in this study.

For the multiplex bead analysis of vitreous fluid, a total of 24 samples were enrolled. Of the 20 patients, 15 (1 man and 14 women) had diagnoses of ocular sarcoidosis for one or both eyes (19 eyes total), based on the international criteria. Vitreous fluid was collected from five eyes of five idiopathic ERM patients (3 men and 2 women), who were enrolled as nonsarcoid controls.

General examinations of all patients were performed by using the algorithm designed for the diagnosis of ocular sarcoidosis.[17]

The group of patients with ocular sarcoidosis comprised 1 man and 14 women; the idiopathic ERM (nonsarcoid control) group comprised 2 men and 3 women. The mean age of the ocular sarcoidosis patients was 66.8 ± 2.2 years, and that of the idiopathic ERM patients was 69.5 ± 3.1 years. Statistical differences were not found in mean age.

Vitreous Sample Collection

Vitreous specimens were obtained from each of 20 patients at the start of a conventional 25-gauge pars plana vitrectomy by using either a CV-24,000 (NIDEK Co., Ltd., Aichi, Japan) or an Accurus (Alcon Laboratories, Inc., Fort Worth, TX) vitrectomy system. A three-way stopcock was attached to the connector on the suction-tube line of the cutter probe, and a 5-ml syringe was connected to the free end of the three-way stopcock. Dry vitrectomy without perfusion of balanced salt solution (Alcon Laboratories, Inc.) was conducted with a cut rate of 500 cpm so as not to damage cells infiltrating into the vitreous. At least 500 μL dry vitreous sample was collected from each patient. Each sample was divided into 5 microtubes for each analysis (200 μL for PCR, 200 μL for multiplex bead analysis, and 100 μL for culture). No intraoperative complications occurred in these patients.

Multiplex Bead Analysis System (Multiplex-ELISA)

The vitreous levels of 27 types of cytokines were determined by using a commercially available multiplex bead analysis system (BioPlex Pro Suspension Array System; BioRad Laboratories, Tokyo, Japan). The 27 cytokines measured were IL-1b; IL-1 receptor antagonist (IL-1ra); IL-2; IL-4; IL-5; IL-6; IL-7; IL-8; IL-9; IL-10; IL-12; IL-13; IL-15; IL-17; eotaxin; basic fibroblast growth factor (bFGF); granulocyte colony-stimulating factor (G-CSF); granulocyte macrophage colony-stimulating factor (GM-CSF); IFN-γ; IFN-γ-IP-10; MCP-1; macrophage inflammatory protein (MIP)-1α and MIP-1β platelet-derived growth factor BB (PDGF-BB); regulated on activation, normal T-cell expressed and secreted (RANTES); tumor necrosis factor α (TNF-α); and VEGF.

Multiplex PCR

Human herpes virus (HHV) genomic DNA was assayed in vitreous fluids by using two independent PCR assays (a qualitative multiplex PCR assay and a quantitative real-time PCR assay) as described previously.[27,28] DNA was extracted from samples by using an E21 virus minikit (QIAGEN, Inc., Valencia, CA) installed on a robotic workstation for automated purification of nucleic acids (BioRobot E21; QIAGEN). Multiplex PCR was designed to qualitatively identify the genomic DNA of the following 8 types of HHV: herpes simplex virus type 1 (HSV-1 or HHV-1) and type 2 (HSV-2 or HHV-2), varicella zoster virus (VZV or HHV-3), Epstein-Barr virus (EBV or HHV-4), cytomegalovirus (CMV or HHV-5), HHV6, HHV7, and HHV8. Other ocular pathogens were also tested, such as *Propionibacterium acnes*, *Toxoplasma*, *Toxocara*, *Bartonella henselae*, *Chlamydia trachomatis*, *Treponema pallidum*, *Mycobacterium tuberculosis*, *Candida* (18s rRNA), *Aspergillus* (18s rRNA), and bacterial 16s rRNA. PCR was performed with a LightCycler (Roche Diagnostics [Schweiz] AG, Rotkreuz, Switzerland). Primers and probes used to detect HHV1 to HHV8 and the PCR conditions have all been described previously.[27] Specific primers for each virus were used with Accuprime *Taq* (Invitrogen, Carlsbad, CA). The templates were subjected to 40 cycles of PCR amplification, and probes were then mixed with the PCR products. Subsequently, real-time PCR was performed only for the HHVs, with the genomic DNA detected by multiplex PCR. The real-time PCR was performed with AmpliTaq Gold (Applied Biosystems, Foster City, CA) and the Real-Time PCR 7300 system (Applied Biosystems). All of the templates obtained were subjected to 45 cycles of PCR amplification. The value of the viral copy number in the sample was considered to be significant when more than 50 copies per tube (5×10^3 copies/mL) were observed.

Macular Thickness Measurement in Ocular Sarcoidosis Patients

The patients who received surgical intervention and cytokine measurements were also evaluated for macular thickness. Macular 3D scans with the spectral-domain 3D-OCT 1000 (TOPCON, Itabashi, Japan) were performed at 1 month after surgery. Patients were divided into two groups on the basis of macular thickness, which was calculated as the average thickness of macular area (fovea 1000 μm across) ± SD. The thin CME range (group 1; 10 patients and 12 eyes) was 119.60 μm to 359.5 μm, and the thick CME range (group 2; 9 patients and 10 eyes) was 359.5 μm to 599.40 μm. Some patients overlapped because of different status of disease in each eye.

Statistical Analysis

Statistical comparisons of the cytokine concentrations of the two patient groups (sarcoidosis and ERM) were carried out by nonparametric analysis with the Mann-Whitney *U* test. The statistical evaluation of the data was performed by using Bonferroni correction. A P value <0.025 was considered to be statistically significant. Statistical comparisons of the macular thickness of three groups (CME grade) were carried out by nonparametric analysis with the Mann-Whitney *U* test.

Results

Vitreous and Serum Levels of 27 Types of Cytokines

The vitreous and serum levels of cytokines are shown in Tables 1 and 2. The levels of PDGF-BB, IL-1ra, IL-4, IL-5, IL-6, IL-8, IL-9, IL-10, IL-12, G-CSF, IFN-γ, IP-10, MCP-1α, MIP-1β, RANTES, TNF-α, and VEGF were significantly higher in the vitreous from patients with ocular sarcoidosis than in that of ERM (non-

TABLE 1. Vitreous Fluid Levels of 27 Types of Cytokines Determined by Using a Multiplex Bead Analysis System

	Sarcoidosis Vitreous, Mean ± SE ($N = 19$)	ERM Vitreous, Mean ± SE ($N = 5$)	*P* Value
PDGF-BB	74.54 ± 12.89	1.29 ± 0.81	0.0043*
IL-1β	0.60 ± 0.08	1.07 ± 0.78	0.1766
IL-1ra	225.1 ± 69.88	7.93 ± 1.76	0.0008†
IL-2	0.885 ± 0.36	0	0.2526
IL-4	0.67 ± 0.09	0.02 ± 0.02	0.0021*
IL-5	0.41 ± 0.07	0.02 ± 0.02	0.0061*
IL-6	736 ± 276.5	13.8 ± 4.2	0.0008†
IL-7	26.93 ± 3.59	9.68 ± 3.27	0.0646
IL-8	161.3 ± 65.95	16.78 ± 7.52	0.0045*
IL-9	28.87 ± 9.04	1.96 ± 1.01	0.0014*
IL-10	13.31 ± 2.79	0.44 ± 0.14	0.0008†
IL-12	33.10 ± 12.02	1.40 ± 1.23	0.0055*
IL-13	45.35 ± 8.74	5.67 ± 4.51	0.0251
IL-15	10.66 ± 1.46	2.68 ± 1.46	0.0257
IL-17	1.49 ± 0.49	0	0.3515
Eotaxin	3.77 ± 0.79	0.49 ± 0.36	0.1409
bFGF	5.98 ± 2.28	2.28 ± 2.28	0.8413
G-CSF	94.88 ± 13.57	7.20 ± 5.70	0.0055*
GM-CSF	130.9 ± 7.63	95.72 ± 10.1	0.088
IFN-γ	57.89 ± 8.69	0.98 ± 0.98	0.0008†
IP-10	58,249 ± 4564	163.5 ± 48.72	0.0008†
MCP-1	1556 ± 232	321.1 ± 48.9	0.0018*
MIP-1α	2.413 ± 0.56	0	0.052
MIP-1β	66.98 ± 9.89	6.06 ± 2.04	0.0008†
RANTES	71.21 ± 15.75	0.52 ± 0.52	0.0017*
TNF-α	17.69 ± 2,12	3.24 ± 1.62	0.0055*
VEGF	155.0 ± 99.59	18.88 ± 17.67	0.0190‡

* More significant difference ($P < 0.01$).
† Most significant difference ($P < 0.001$).
‡ Significant difference ($P < 0.025$).

TABLE 2. Serum Levels of 27 Types of Cytokines Determined by Using a Multiplex Bead Analysis System

	Sarcoidosis Vitreous, Mean ± SE ($N = 19$)	ERM Serum, Mean ± SE ($N = 5$)	*P* Value
PDGF-BB	8703 ± 511.7	8526 ± 1857	0.887
IL-1β	3.72 ± 0.58	5.91 ± 1.91	0.2268
IL-1ra	206.9 ± 22.42	223.3 ± 42.87	0.887
IL-2	5.12 ± 3.04	54.21 ± 49.40	0.721
IL-4	6.96 ± 1.25	5.76 ± 2.04	0.4342
IL-5	2.76 ± 0.23	25.99 ± 23.60	0.8868
IL-6	28.51 ± 10.50	116.1 ± 67.50	0.1355
IL-7	9.79 ± 0.89	8.12 ± 2.45	0.3935
IL-8	415.7 ± 193.3	791.3 ± 340.3	0.2554
IL-9	115.7 ± 51.05	59.81 ± 22.51	0.5695
IL-10	5.325 ± 0.91	5.43 ± 1.64	0.8869
IL-12	40.26 ± 6.12	83.49 ± 46.87	0.6698
IL-13	5.98 ± 1.59	7.79 ± 3.54	0.4772
IL-15	0	1.522 ± 1.27	0.0061*
IL-17	55.23 ± 8.65	48.43 ± 13.96	0.4339
Eotaxin	117.80 ± 18.12	117.0 ± 28.97	0.9433
bFGF	23.11 ± 5.93	43.42 ± 21.66	0.5426
G-CSF	28.46 ± 4.19	28.52 ± 8.69	1
GM-CSF	8.56 ± 2.67	77.93 ± 62.45	0.1803
IFN-γ	63.06 ± 7.97	124.9 ± 62.16	0.6187
IP-10	3485 ± 555.2	1053 ± 108.3	0.0105†
MCP-1	47.02 ± 10.83	64.83 ± 29.95	1
MIP-1α	68.39 ± 31.38	269.9 ± 161.6	0.1176
MIP-1β	752.7 ± 171.5	1777 ± 789.1	0.2007
RANTES	4318 ± 180.5	5077 ± 520.2	0.1768
TNF-α	52.21 ± 8.79	172.2 ± 76.81	0.0941
VEGF	103.9 ± 13.71	109.4 ± 30.01	0.9433

* More significant difference ($P < 0.01$).
† Significant difference ($P < 0.025$).

sarcoid control) patients. Interestingly, although the levels of these cytokines were much higher in vitreous fluid of patients with ocular sarcoidosis, the differences in the serum cytokine levels between these two groups (with only two exceptions) were not significant. Serum IP-10 was significantly higher in patients with ocular sarcoidosis than in those with ERM, but the serum levels of IL-15 were significantly lower than in patients with ERM.

The cytokine ratios of vitreous/serum in ocular sarcoidosis and ERM are shown in Table 3. The vitreous/serum ratios of PDGF-BB, IL-1ra, IL-4, IL-5, IL-6, IL-12, IL-13, G-CSF, IFN-γ, IP-10, MCP-1, MIP-1β, RANTES, TNF-α, and VEGF were significantly higher in ocular sarcoidosis samples than in those of ERM (nonsarcoid control) patients.

The Relationship between Postoperative Macular Thickness and Cytokine Concentrations

Data from the analysis of vitreous cytokines were compared with macular thickness 1 month after surgery (Fig.). Macular thickness in group 1 (10 patients and 12 eyes) was <359.5 μm, whereas measurements in group 2 (9 patients and 10 eyes) were ≥359.5 μm. The levels of most cytokines tend to increase in patients within the thin CME group. Notably, IL-1ra ($P = 0.02$), IL-2 ($P = 0.03$), IL-4 ($P = 0.03$), IL-8 ($P = 0.03$), IFN-γ ($P = 0.03$), IP-10 ($P = 0.01$), MCP-1 ($P = 0.03$), MIP-1β ($P = 0.005$), and RANTES ($P = 0.006$) were significantly upregulated in group 1. In contrast, the levels of PDGF-BB, IL-12, IL-13, bFGF, G-CSF, and VEGF seemed to be elevated in group 2 (no statistical difference).

DISCUSSION

To the best of the authors' knowledge, this is the first study to investigate both vitreous and serum levels of cytokines, using multiplex ELISA analysis, in patients with ocular sarcoidosis. These patients had high levels of several types of cytokines, especially T helper 1 (Th-1)–related cytokines, in their vitreous body. In their investigation of the relationship between cytokine and clinical stage, the authors noticed that advanced pathologic stage in the posterior segment (e.g., complications such as severe CME) might be influenced by G-CSF, VEGF, and PDGF-BB, which are highly associated with vascular leakage, as previously reported.[29,30] In fact, only the cytokines that are associated with vascular permeability tended to undergo upregulation in the advanced CME stage. Previous reports have suggested that VEGF is strongly associated with blood-retina barrier (BRB) breakdown.[18] In contrast, almost all of the proinflammatory cytokines were downregulated in vitreous fluid from patients with advanced-stage ocular sarcoidosis (Fig.). It appears that numerous cytokines may be increased in order to increase the lymphocyte infiltration in vitreous fluid or macrophage infiltration into granulomas at the retinal layer. There is the potential for an increase in BRB breakdown from the high vitreous/serum ratio of cytokines, such as PDGF-BB, IL-6, G-CSF, and VEGF; if so, all inflammatory and angiogenic cytokine levels should increase in vitreous fluid after onset of

TABLE 3. Vitreous/Serum Ratio of 27 Types of Cytokines

	Sarcoidosis Vitreous/Serum, Mean ± SE ($N = 19$)	ERM Vitreous/Serum, Mean ± SE ($N = 5$)	*P* Value
PDGF-BB	0.006 ± 0.001	0.0001 ± 0.000009	0.0054*
IL-1β	0.61 ± 0.33	0.22 ± 0.20	0.0753 ns
IL-1ra	2.59 ± 1.26	0.03 ± 0.01	0.0022*
IL-2	4.45 ± 2.83	0	0.1470 ns
IL-4	0.39 ± 0.14	0.002 ± 0.002	0.0017*
IL-5	0.21 ± 0.03	0.01 ± 0.01	0.0096*
IL-6	90.69 ± 25.11	0.93 ± 0.72	0.0018*
IL-7	2.97 ± 0.59	1.91 ± 0.79	0.3555
IL-8	4.31 ± 1.29	0.09 ± 0.05	0.0229 ns
IL-9	1.54 ± 0.81	0.04 ± 0.03	0.0262 ns
IL-10	15.44 ± 8.79	4.49 ± 4.46	0.0283 ns
IL-12	1.12 ± 0.44	0.008 ± 0.005	0.0015*
IL-13	21.53 ± 8.94	0.53 ± 0.24	0.0129†
IL-15	Impossible to measure	0	Not measured
IL-17	0.36 ± 0.27	0	0.6944 ns
Eotaxin	0.36 ± 0.27	0	0.6944 ns
bFGF	0	0	ns
G-CSF	12.83 ± 5.06	0.27 ± 0.13	0.0028*
GM-CSF	21.86 ± 5.08	9.88 ± 7.57	0.1631 ns
IFN-γ	1.88 ± 0.61	0.02 ± 0.02	0.0008‡
IP-10	24.64 ± 3.86	0.13 ± 0.05	0.0008‡
MCP-1	58.14 ± 15.07	12.62 ± 5.51	0.0157†
MIP-1α	0.17 ± 0.05	0	0.0787
MIP-1β	0.20 ± 0.04	0.013 ± 0.01	0.0028*
RANTES	0.02 ± 0.004	0.0001 ± 0.0001	0.0017*
TNF-α	0.38 ± 0.09	0.03 ± 0.03	0.0017*
VEGF	0.81 ± 0.30	0.01 ± 0.007	0.0025*

ns, not specified.
* More significant difference ($P < 0.01$).
† Significant difference ($P < 0.025$).
‡ Most significant difference ($P < 0.001$).

the clinical condition. Moreover, the cytokine level in vitreous fluid for herpes virus or parasite infection, which might be associated with high BRB breakdown, was much higher than that for both nonocular sarcoidosis and ocular sarcoidosis. However, the number of groups studied is too limited to allow a comprehensive discussion for the present experiment. Further investigations should be performed to analyze the BRB breakdown, with comparison between blood and vitreous albumin concentration.

Interestingly, IP-10 was the only cytokine that was found to be elevated in both the vitreous body and serum of sarcoid uveitis patients. IP-10, also known as C-X-C motif chemokine 10, is a chemokine that is induced by IFN-γ and secreted from monocytes and macrophages stimulated with IFN-γ. Because IP-10 promotes the migration of T cells to sites of inflammation, it is an attractive candidate for further investigation of the mechanisms promoting the development of sarcoid granulomas. IP-10 is strongly expressed in sarcoid granuloma tissue,[26] and IP-10 secretion from alveolar macrophages is highly correlated with the $CD4^+$ T lymphocyte population. This finding may indicate that IP-10 secreted from macrophages in the granuloma tissue can regulate migration of $CD4^+$ T lymphocytes to the site of sarcoidosis during inflammatory processes in the posterior segment of the eye. The amount of $CD4^+$ T lymphocytes is related to IP-10 levels in BALF[26]; the authors observed a similar phenomenon in vitreous fluid samples in an ongoing experiment (manuscript submitted). The vitreous fluid from patients with ocular sarcoidosis had high amounts of $CD4^+$ T lymphocytes, but not $CD8^+$ T lymphocytes (data not shown; manuscript submitted). Reportedly, serum levels of IP-10 in patients with sarcoidosis were significantly higher than those of healthy volunteers; however, peripheral blood mononuclear cells did not increase the IP-10 production.[31] The present data indicated that IP-10 might be secreted from local macrophages that had infiltrated granuloma tissue in retina, vitreous fluid, or any other place in the body. In fact, the authors found that retinas from patients with sarcoid uveitis involved granulomas that contained $CD68^+$ macrophages (data not shown). Therefore, serum levels of IP-10 probably reflect the clinical state of sarcoid uveitis. High levels of Th-1-type cytokines in vitreous fluid suggest that IP-10 cooperates with Th-1-type cytokines, which act as local factors that promote T cell activation and proliferation.

Several cytokines have angiogenic/vascular permeability properties; for example, IL-6 increases vascular permeability.[32] Moreover, VEGF is a well-known angiogenic factor that is highly associated with vascular leakage in retinas of patients suffering with diabetic retinopathy, retinal vascular occlusion, or ROP. Vitreous levels of VEGF are significantly higher in eyes of patients with proliferative ROP than in those of control individuals, and VEGF is the only cytokine for which the vitreous level is correlated with vascular activity in ROP eyes.[33] Here, the authors intended to determine which cytokine(s) were correlated with critical clinical issues, such as the development of macular edema. The authors found that vitreous cytokines that are proangiogenic and/or associated with vascular leakage, such as VEGF, PDGF-BB, and G-CSF, tended to be upregulated in patients with severe macular edema (group 2), but not in patients with thin macular edema (group 1). In contrast, other proinflammatory and proangiogenic cytokines, such as MCP-1,[34] RANTES, IL-1ra,[35] and TNF-α,[36] which are all associated with vascular permeability, were downregulated in patients with severe macular edema. Moreover, IP-10, which has antiangiogenic properties, was significantly higher in the vitreous fluid of group 1 than in that of group 2. IP-10 prevents corneal hemangiogenesis[37] and inhibits growth and metastasis of lung carcinoma[38]; based on these findings, it is thought that high VEGF concentrations in vitreous fluids may be associated with macular edema and may enhance chronic inflammation. Furthermore, the balance of both proangiogenic and antiangiogenic cytokines was maintained until severe macular edema developed. Most patients in group 2 were treated with long-term steroids, or abandoned disease status before surgery. The visual acuity did not improve after surgery, most likely because of irreversible change of the sensory retina caused by long-standing macular edema (data not shown). Surprisingly, even in the patients who were treated with steroids before surgery, the vitreous fluid had higher cytokine levels than the vitreous fluid from the control group. The results suggest that proinflammatory cytokines that are upregulated in the vitreous fluid of ocular sarcoidosis patients might be influenced by BRB breakdown. It proved problematic to test for this in the present study because the limited amount of vitreous sample precluded comparison between serum and vitreous protein; however, VEGF, PDGF-BB, and G-CSF levels should be increased in primary status, not in the late stage of disease such as in group 2. Therefore, the authors believe that surgical intervention should be performed at an early stage of macular edema (before development of severe macular edema) for the purpose of removing proinflammatory cytokines from vitreous fluid.

Previous reports have shown that surgical intervention is beneficial for improvement of CME or ERM caused by sarcoid uveitis.[39,40] Here, the authors performed vitrectomy for acute-phase uveitis without CME or ERM. Diamond and Kaplan[41]

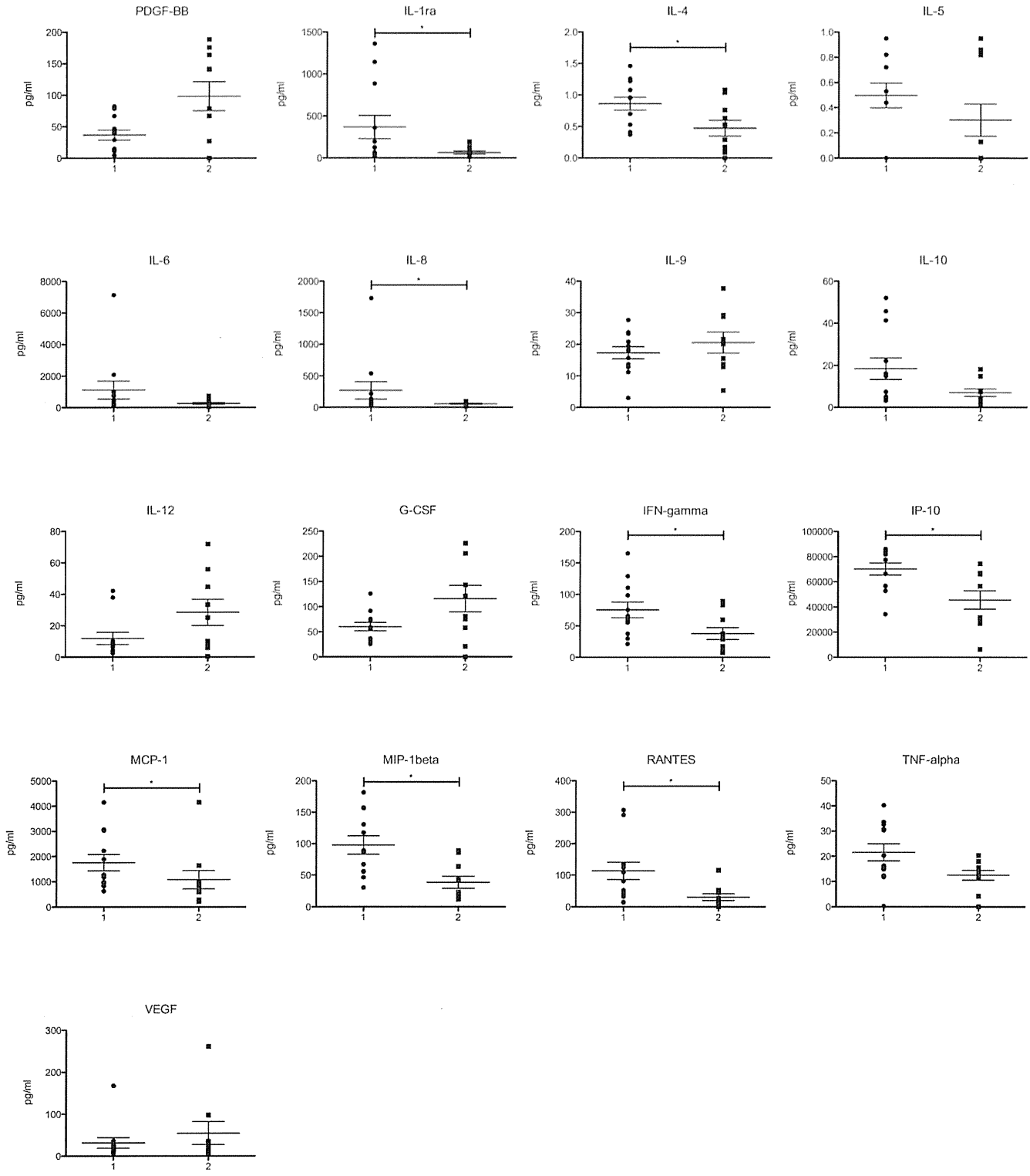

Figure. The relationship between postoperative macular thickness and cytokine concentration in vitreous fluid at 1 month after operation. The y-axis indicates the concentration of cytokines in vitreous fluid (pg/mL). The x-axis indicates the level of macular thickness. Patients were divided into two groups by macular thickness (average thickness of macular area [fovea 1000 μm across] ± DEV): thin CME range (1 = group 1) from 119.60 μm to 359.5 μm and thick CME range (2 = group 2) from 359.5 μm to 599.40 μm. Some patients overlapped because of different status of disease in each eye. *$P < 0.05$.

have suggested that removal of inflammatory mediators (such as T cells) that accumulate in vitreous fluid in patients with uveitis may have a beneficial effect on macular edema. Likewise, the present study showed that removal of inflammatory cells and cytokines may lead to suppression of ocular inflammation. This report demonstrated that several proinflammatory cytokines persist at highly elevated levels in the vitreous fluid of patients with ocular sarcoidosis. Moreover, the authors confirmed that $CD4^+$ T cells also infiltrated into the vitreous fluid of patients with sarcoid uveitis (manuscript submitted).

The authors found that the retinal granulomas also had *P. acnes* DNA (data not shown). As with pulmonary sarcoidosis, the infectious theory should be considered for the etiology of ocular sarcoidosis. However, because the sample number was limited, further investigations and proper control samples are required to elucidate the role of *P. acnes* in ocular sarcoidosis. Therefore, eliminating the continuous exposure to proinflammatory cytokines, proinflammatory cells, and infectious agents (which were the key factors for inducing macular edema) by surgical intervention should be a beneficial treatment for preventing progression of uveitis. On the other hand, some anti-inflammatory cytokines, such as IL-4 and RANTES, were also upregulated in vitreous fluid in the present cases. These cytokines seemed to increase in moderate inflammatory status either to balance the Th1 and Th2 status, or to recruit the T regulatory cells for suppressing inflammation. Notably, RANTES is likely to be a key chemokine for suppressing inflammation in an experimental autoimmune uveitis model for recruiting anti-inflammatory $CD8^+$ T cells.[42] However, in this study, the number of vitreous $CD8^+$ T lymphocytes did not differ significantly in patients who had high RANTES level in vitreous fluid (data not shown). Because the number of patients was limited in this study, further studies are required to investigate and analyze the relationship between RANTES level and $CD8^+$ T lymphocytes in vitreous fluid.

The limitations of this study include the lack of an accurate control group and the variability in the duration of postoperative follow-up. In comparison, the level of IL-1β in the vitreous in infectious uveitis (153.24 ± 117.33 pg/mL) was significantly higher than in ocular sarcoidosis (0.60 ± 0.08 pg/mL; $P < 0.01$). However, no specific elevation of cytokine was found in ocular sarcoidosis. Further investigations should be performed to analyze the specific elevation of cytokine in ocular sarcoidosis. Despite this, these findings strongly suggest that highly elevated levels of proinflammatory cytokines are present in the vitreous fluid of patients with sarcoid uveitis, and that surgical intervention may be beneficial by removing excess proinflammatory cytokines from the vitreous fluid. Further investigations are warranted.

Acknowledgments

The authors thank Kentaro Kojima, Hideki Komori, and Toru Yasuhara for the helpful sample collections. Moreover, the authors thank Wendy Chao for editing and critical reading of this manuscript.

References

1. Baughman RP, Lower EE, du Bois RM. Sarcoidosis. *Lancet*. 2003;361:1111-1118.
2. Margolis R, Lowder CY. Sarcoidosis. *Curr Opin Ophthalmol*. 2007;18:470-475.
3. Nunes H, Bouvry D, Soler P, Valeyre D. Sarcoidosis. *Orphanet J Rare Dis*. 2007;2:46.
4. Wu JJ, Schiff KR. Sarcoidosis. *Am Fam Physician*. 2004;70:312-322.
5. Rothova A. Ocular involvement in sarcoidosis. *Br J Ophthalmol*. 2000;84:110-116.
6. Statement on sarcoidosis: Joint Statement of the American Thoracic Society (ATS), the European Respiratory Society (ERS) and the World Association of Sarcoidosis and Other Granulomatous Disorders (WASOG) adopted by the ATS Board of Directors and by the ERS Executive Committee, February 1999. *Am J Respir Crit Care Med*. 1999;160:736-755.
7. Hiraga Y. An epidemiological study of clustering of sarcoidosis cases [in Japanese]. *Nippon Rinsho*. 1994;52:1438-1442.
8. Hosoda Y, Hiraga Y, Odaka M, et al. A cooperative study of sarcoidosis in Asia and Africa: analytic epidemiology. *Ann N Y Acad Sci*. 1976;278:355-367.
9. McGrath DS, Goh N, Foley PJ, du Bois RM. Sarcoidosis: genes and microbes—soil or seed? *Sarcoidosis Vasc Diffuse Lung Dis*. 2001;18:149-164.
10. Ishige I, Usui Y, Takemura T, Eishi Y. Quantitative PCR of mycobacterial and propionibacterial DNA in lymph nodes of Japanese patients with sarcoidosis. *Lancet*. 1999;354:120-123.
11. Yasuhara T, Tada R, Nakano Y, et al. The presence of Propionibacterium spp. in the vitreous fluid of uveitis patients with sarcoidosis. *Acta Ophthalmol Scand*. 2005;83:364-369.
12. Lynch JP III, Sharma OP, Baughman RP. Extrapulmonary sarcoidosis. *Semin Respir Infect*. 1998;13:229-254.
13. Crick RP, Hoyle C, Smellie H. The eyes in sarcoidosis. *Br J Ophthalmol*. 1961;45:461-481.
14. Ohara K, Okubo A, Sasaki H, Kamata K. Intraocular manifestations of systemic sarcoidosis. *Jpn J Ophthalmol*. 1992;36:452-457.
15. Jabs DA, Johns CJ. Ocular involvement in chronic sarcoidosis. *Am J Ophthalmol*. 1986;102:297-301.
16. Bonfioli AA, Orefice F. Sarcoidosis. *Semin Ophthalmol*. 2005;20:177-182.
17. Herbort CP, Rao NA, Mochizuki M. International criteria for the diagnosis of ocular sarcoidosis: results of the first International Workshop On Ocular Sarcoidosis (IWOS). *Ocul Immunol Inflamm*. 2009;17:160-169.
18. Yoshimura T, Sonoda KH, Sugahara M, et al. Comprehensive analysis of inflammatory immune mediators in vitreoretinal diseases. *PLoS One*. 2009;4:e8158.
19. Kezuka T, Sakai J, Usui N, Streilein JW, Usui M. Evidence for antigen-specific immune deviation in patients with acute retinal necrosis. *Arch Ophthalmol*. 2001;119:1044-1049.
20. Sato T, Kusaka S, Shimojo H, Fujikado T. Simultaneous analyses of vitreous levels of 27 cytokines in eyes with retinopathy of prematurity. *Ophthalmology*. 2009;116:2165-2169.
21. de Boer JH, van Haren MA, de Vries-Knoppert WA, et al. Analysis of IL-6 levels in human vitreous fluid obtained from uveitis patients, patients with proliferative intraocular disorders and eye bank eyes. *Curr Eye Res*. 1992;11(suppl):181-186.
22. Ongkosuwito JV, Feron EJ, van Doornik CE, et al. Analysis of immunoregulatory cytokines in ocular fluid samples from patients with uveitis. *Invest Ophthalmol Vis Sci*. 1998;39:2659-2665.
23. Curnow SJ, Falciani F, Durrani OM, et al. Multiplex bead immunoassay analysis of aqueous humor reveals distinct cytokine profiles in uveitis. *Invest Ophthalmol Vis Sci*. 2005;46:4251-4259.
24. Banerjee S, Savant V, Scott RA, Curnow SJ, Wallace GR, Murray PI. Multiplex bead analysis of vitreous humor of patients with vitreoretinal disorders. *Invest Ophthalmol Vis Sci*. 2007;48:2203-2207.
25. Yoshimura T, Sonoda KH, Ohguro N, et al. Involvement of Th17 cells and the effect of anti-IL-6 therapy in autoimmune uveitis. *Rheumatology (Oxford)*. 2009;48:347-354.

26. Agostini C, Cassatella M, Zambello R, et al. Involvement of the IP-10 chemokine in sarcoid granulomatous reactions. *J Immunol.* 1998;161:6413–6420.
27. Sugita S, Shimizu N, Watanabe K, et al. Use of multiplex PCR and real-time PCR to detect human herpes virus genome in ocular fluids of patients with uveitis. *Br J Ophthalmol.* 2008; 92:928–932.
28. Miyanaga M, Sugita S, Shimizu N, et al. A significant association of viral loads with corneal endothelial cell damage in cytomegalovirus anterior uveitis. *Br J Ophthalmol.* 2010;94: 336–340.
29. Mishra BB, Poulter LW, Janossy G, James DG. The distribution of lymphoid and macrophage like cell subsets of sarcoid and Kveim granulomata: possible mechanism of negative PPD reaction in sarcoidosis. *Clin Exp Immunol.* 1983;54:705–715.
30. Yao H, Duan M, Buch S. Cocaine-mediated induction of platelet-derived growth factor: implication for increased vascular permeability. *Blood.* 2011;117:2538–2547.
31. Mishra BB, Poulter LW, Janossy G, Sherlock S, James DG. The Kveim-Siltzbach granuloma: a model for sarcoid granuloma formation. *Ann N Y Acad Sci.* 1986;465:164–175.
32. Funatsu H, Yamashita H, Ikeda T, Mimura T, Eguchi S, Hori S. Vitreous levels of interleukin-6 and vascular endothelial growth factor are related to diabetic macular edema. *Ophthalmology.* 2003;110:1690–1696.
33. Mizuki N, Ohno S, Sato T, et al. Microsatellite polymorphism between the tumor necrosis factor and HLA-B genes in Behcet's disease. *Hum Immunol.* 1995;43:129–135.
34. Papadia M, Herbort CP, Mochizuki M. Diagnosis of ocular sarcoidosis. *Ocul Immunol Inflamm.* 2010;18:432–441.
35. Ishihara M, Ishida T, Mizuki N, Inoko H, Ando H, Ohno S. Clinical features of sarcoidosis in relation to HLA distribution and HLA-DRB3 genotyping by PCR-RFLP. *Br J Ophthalmol.* 1995;79:322–325.
36. Rosenberg GA, Estrada EY, Dencoff JE, Stetler-Stevenson WG. Tumor necrosis factor-alpha-induced gelatinase B causes delayed opening of the blood-brain barrier: an expanded therapeutic window. *Brain Res.* 1995;703:151–155.
37. Proost P, Schutyser E, Menten P, et al. Amino-terminal truncation of CXCR3 agonists impairs receptor signaling and lymphocyte chemotaxis, while preserving antiangiogenic properties. *Blood.* 2001;98:3554–3561.
38. Arenberg DA, Kunkel SL, Polverini PJ, et al. Interferon-gamma-inducible protein 10 (IP-10) is an angiostatic factor that inhibits human non-small cell lung cancer (NSCLC) tumorigenesis and spontaneous metastases. *J Exp Med.* 1996;184: 981–992.
39. Kiryu J, Kita M, Tanabe T, et al. Pars plana vitrectomy for epiretinal membrane associated with sarcoidosis. *Jpn J Ophthalmol.* 2003;47:479–483.
40. Kiryu J, Kita M, Tanabe T, Yamashiro K, Miyamoto N, Ieki Y. Pars plana vitrectomy for cystoid macular edema secondary to sarcoid uveitis. *Ophthalmology.* 2001;108:1140–1144.
41. Diamond JG, Kaplan HJ. Lensectomy and vitrectomy for complicated cataract secondary to uveitis. *Arch Ophthalmol.* 1978;96:1798–1804.
42. Sonoda KH, Sasa Y, Qiao H, et al. Immunoregulatory role of ocular macrophages: the macrophages produce RANTES to suppress experimental autoimmune uveitis. *J Immunol.* 2003; 171:2652–2659.